Characterizing the Groundwater-Surface Water Interactions in Different Subsurface Geologic Environments Using Geochemical and Isotopic Analyses

By

Molly M. Long

Submitted to the graduate degree program in Geology
and the Graduate Faculty of the University of Kansas in partial fulfillment of the
requirements for the degree of Master of Science.

_____
Chairperson Randy Stotler

_____
Jennifer Roberts

_____
Leigh A. Stearns

_____
Donald Whittemore

Date Defended: August 15, 2014

The Thesis Committee for Molly M. Long

certifies that this is the approved version of the following thesis:

Characterizing the Groundwater-Surface Water Interactions in Different Subsurface Geologic Environments Using Geochemical and Isotopic Analyses

_____

Chairperson Randy Stotler

Date approved: August 20, 2014

## Abstract

Shallow aquifers located near streams can be affected by groundwater contamination as a result of recharge from surface water; however, stream stage variation, subsurface geology, and seasonal changes can alter the magnitude of groundwater-surface water interactions. Knowledge of the influence these factors have on surface water connections with groundwater will help determine possible recharge and contaminant flow paths affecting future water supply wells installed in similar alluvial environments. This research capitalized on previously collected physical data, including geology, water-level measurements, and hydraulic conductivity, as well as new physical, geochemical, and isotopic data to assess the effects of hydrogeological and seasonal conditions on groundwater-surface water interactions at two geologically distinct field sites.

Groundwater level measurements and surface and groundwater samples were collected at both field sites during the growing and non-growing seasons to assess changes in groundwater-surface water interactions. Water samples were collected from wells in sands and gravels of the alluvial aquifer and the deeper High Plains aquifer that are separated by a clay aquitard in a river valley at the Larned Research Site (LRS) in central Kansas. Water was sampled from a small stream and wells at different depths in alluvium overlying a shallow limestone bedrock aquifer at the Rock Creek Site (RCS) in southeastern Kansas. Dissolved inorganic concentrations and $\delta^{2}H$ and $\delta^{18}O$ isotope compositions were determined for all samples to indicate the influence of changing stream stage and geology on groundwater-surface water interactions.

Water from the aquitard wells at the LRS had considerably lower dissolved solid concentrations compared to the shallow and deep aquifer wells. The isotopic compositions became lighter with depth from the shallow to deep aquifer samples, but were lightest in the

aquitard samples. The isotopic compositions of the precipitation and groundwater indicate that surface water recharge to the aquifers is likely to occur primarily in the spring and summer. The disparity between the aquifers and aquitard samples implied older, fresher water contained in a leaky aquitard system. The low hydraulic conductivity of the aquitard acts as a geologic barrier, although heterogeneities of the leaky aquitard apparently connect the two aquifers. The good hydrologic connection between the alluvial aquifers and the river bed acts as a contamination pathway for groundwater under the direct influence of surface water, whereas the aquitard protects the High Plains aquifer from rapid contamination by surface water.

At the RCS, selected dissolved constituent concentrations in groundwater near the water table varied seasonally in two water table wells with evidence of lateral flow to and from the stream. In contrast, groundwater in the alluvium base wells, located at the base of the silty-clay alluvium and top of the weathered limestone, and in a bedrock well generally exhibited similar geochemical and isotopic values. The geochemical and isotopic differences between the stream and two water-table well samples and the remaining water-table, alluvium base, and bedrock well samples suggest different groundwater storage times at the RCS. The geochemical and isotopic values for groundwater from the two water-table wells best connected to the stream varied with changing stream stage and season, indicating short-term storage compared to the consistency of the deeper groundwater, which represented longer-term storage. Surface water recharge pathways at the RCS, which could function as recharge or contamination pathways, vary substantially as a result of the heterogeneous subsurface geology, but only appear to substantially affect selected portions of groundwater near the water table. The shallow bedrock aquifer is protected from contamination by the silty-clay alluvium.

## Acknowledgments

First and foremost, I would like to thank Kent Crawford for taking a chance on a high school student and introducing me to the world of hydrology and water quality. Without your help and encouragement, my interest in hydrogeology would have never risen above 'base flow.'

My family and friends were my 'solid bedrock' in the consistently changing flow paths of the academic world. My mother, father, and sister have supported me throughout all my research efforts since I discovered passion for science. A special thank you is given to Joyce and Willie as well as Alyssa, Britney, DJ, Erica, and Tyler for large amounts of encouragement and patience. Additionally, I want to give a shout-out to the Hydro-Group of Angela, Brant, Britney, Brooks, Carolyn, David, and Michael.

The support I received from everyone in the Department of Geology at the University of Kansas and the Kansas Geological Survey was instrumental, and I cannot thank everyone enough. Thank you to Greg Cane, Ed Reboulet, Masato Ueshima, and all my committee members. This project could not have been completed without funding provided by the Kansas Geological Survey, Department of Geology at the University of Kansas, and Association for Women in Geosciences Osage Chapter.

A special thank you is given to Don Whittemore for your guidance and optimism during the writing process and field sampling trips. Thank you to Randy Stotler for support and re-assurance throughout the entire graduate school process.

Finally, thank you to Florida Georgia Line, Luke Bryan, and Eli Young Band; without those country artists and associated albums, the late nights would have seemed even later.

# Table of Contents

## List of Tables



## List of Figures

# Chapter 1: Introduction

Alluvial aquifers are utilized to support a large number of water supply wells based on high productivity, accessibility, and the well development process (Choi et al., 2009; Ray et al., 2002; Teles et al., 2004). The integrity of some shallow aquifers located near streams has been compromised by contamination resulting from surface water recharge, including the pathogen contamination of groundwater under the direct influence of surface water recharge in Walkerton, Canada (Alley et al., 1999; McCarthy et al., 1992; O'Connor, 2002; Schubert, 2002; Sheets et al., 2002; USEPA, 1998; Winter et al., 1998). As the general importance of groundwater resources increases, knowledge of the factors affecting surface water recharge to groundwater, such as stream stage, subsurface geology, and seasonality, will help predict the potential of surface water as a significant source of aquifer recharge and possible contamination pathways (McCarthy et al., 1992; Schubert, 2002; Winter et al., 1998).

Surface water movement into an aquifer varies based on changes in stream stage (Alley et al., 2002; Schubert, 2002). Stream stage increases with precipitation events and snowmelt and allows surface water to recharge the water table through the floodplain and stream bank infiltration (Ray et al., 2002; Winter et al., 1998). Deeper aquifer recharge is dependent on large and extended rainfall events where precipitation can percolate in both uplands and valleys into groundwater aquifers before evapotranspiration can occur (Vries and Simmers, 2002). As stream stage recedes, seepage from the elevated water table adjacent to the stream will recharge the stream (Winter et al., 1998). Depending on the flow paths and hydraulic conductivities of the alluvium, groundwater recharged by surface water can remain in an aquifer anywhere between a few weeks to years (Winter et al., 1998).

Subsurface heterogeneities alter groundwater-surface water interactions by modifying hydrologic flow paths, which can be geochemically monitored. During alluvial aquifer formation, adjustments in channel structures, maturing river stages, and changes in deposition can occur (Teles et al., 2004). The result is a complex, heterogeneous subsurface geometry where connections between groundwater and surface water can be traced by integrating geochemical and isotopic analyses of water samples (e.g. Aji et al., 2008; Gleeson et al., 2005; Ladouche et al., 2001). Geochemical interpretations of surface and groundwater interactions can be limited by an incomplete understanding of biogeochemical reactions and dilution effects in the studied area (McCarthy et al., 1992). Stable isotope compositions provide an additional method of observing these connections based on distinguishable surface water, groundwater, and precipitation isotopic signatures (Gibson et al., 2005; Krabbenhoft et al., 1990). The combined geochemical and isotopic trends in groundwater and surface water can reveal geologic subsurface heterogeneities between the two water sources.

Seasonal variations observed in surface and groundwater geochemistry can be used to identify changes in surface water and groundwater interactions. In particular, deuterium and oxygen-18 isotopic compositions of precipitation vary between seasons, with winter precipitation being more depleted in heavy isotopes compared to summer precipitation (e.g. Darling et al., 2003; Gibson et al., 2005; Kendall and Coplen, 2001). Shallow groundwater isotope compositions generally fluctuate around the mean annual isotopic compositions of precipitation; deviations from the mean are due to seasonal infiltration changes. The magnitude of these variations decreases with depth based on the critical zone theory (Clark and Fritz, 1997). Groundwater distribution and mean residence time, movement of precipitation through the hydrological cycle, and seasonal recharge can be determined from these seasonal fluctuations of

isotope compositions (Darling et al., 2003; Gibson et al., 2005; Huddart et al., 1999; Kendall and Coplen, 2001; McGuire et al., 2002; Reddy et al., 2006).

This research capitalizes on existing infrastructure at two established field sites with differing stream stage and lithology to assess disparities in groundwater-surface water interactions. At each research site, connections between surface water and groundwater should vary relative to stream stage, subsurface geology, and seasonal changes. Newly collected surface and groundwater geochemical and isotopic data, combined with newly and previously collected physical data, will help show how geological and seasonal conditions affect groundwater-surface water interactions. These data indicate the influence, or lack thereof, of surface water on groundwater, and aid in identifying recharge pathways and aquifer vulnerability to contamination.

# Chapter 2: Materials and Methods

## Site Descriptions

Two research sites established by the Kansas Geological Survey, the Larned Research Site (LRS) and the Rock Creek Site (RCS), were chosen based on differing subsurface geologic environments and hydrologic pathways, the presence of existing infrastructure, and somewhat different climate (Figure 1).

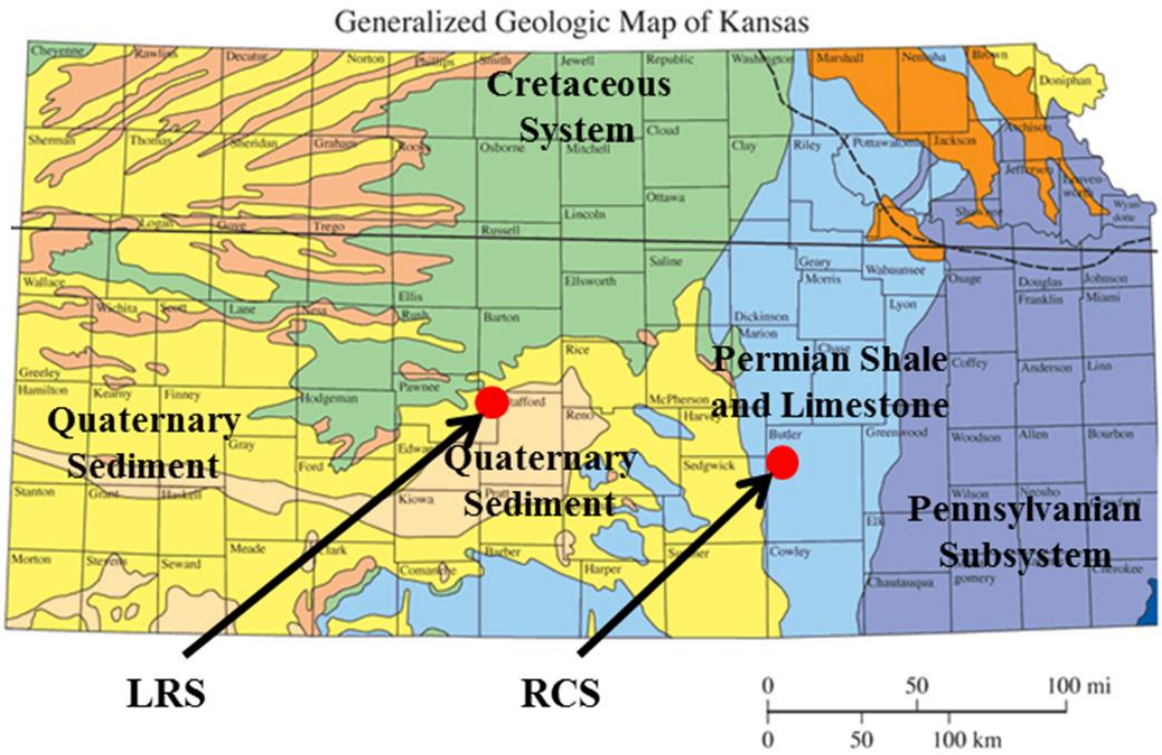


Figure 1. Location of the two sample sites in Kansas: the Larned Research Site (LRS) and the Rock Creek Site (RCS) (modified from Kansas Geological Survey, 1996).

The LRS is located in Pawnee County, Kansas next to the Arkansas River (Figure 1). The Arkansas River was not flowing during the study period of November 2012 through October 2013; a drought affected the area for a couple years prior to sampling. The dry river bed is composed of loose, coarse sand and gravel (Appendix I). Previous river flow in the Arkansas River was dependent on flooding from two water sources: the high salinity water from Colorado and fresher high flows from the Pawnee River (Whittemore et al., 2005). The mean annual precipitation is about 610 mm/yr at the study site. The riparian zone surrounding the river bed is mainly vegetated by cottonwoods, mulberries, and willows (Butler et al., 2007). The effects of riparian vegetation on water levels in wells in the shallow alluvial aquifer and the deeper High Plain aquifer at the LRS have been monitored for over a decade (e.g., Butler et al., 2007). The water-level fluctuations observed in the wells vary spatially and temporally in response to the

quantity and type of riparian cover and hydraulic properties of the subsurface stratigraphy. Higher densities of riparian vegetation correspond to increased evapotranspiration and variations of well water levels. The evapotranspiration of the riparian vegetation results in diurnal variations in groundwater levels; the magnitude of the variation is dependent on climatic conditions, including global irradiance and air temperature; higher irradiance and temperature correspond to a greater magnitude of water-level diurnal cycles.

Butler et al. (2004) utilized direct-push methods to characterize the stratigraphy of the sediments at the LRS. The subsurface includes a shallow alluvial aquifer and a deep aquifer, the High Plains aquifer (HPA), separated by a low permeability aquitard (Figure 2). The shallow phreatic alluvial aquifer, approximate thickness of 9.1 m, is composed of coarse sand and gravel, to silt and clay (Butler et al., 2004; Whittemore et al., 2012). The aquifer also contains irregularly distributed clay lenses concentrated in the lower portion of the aquifer (Butler et al., 2004). Several observation wells are screened at different depths in the alluvial aquifer and located at varying distances from the river channel (Figure 5, Table 1). A pumping test performed by Butler et al. (2004) on a well screened in the shallow aquifer indicated an approximate transmissivity of 353 $m^2$/d, specific yield of 0.31, and that the water-table aquifer is in hydraulic connection with the periodically flowing Arkansas River. During the pumping test, the geochemical concentrations varied in the water pumped from the phreatic alluvial aquifer well. The specific conductivity measurements generally remained constant throughout the test at roughly 1,330 μS/cm. After an initial decrease of 0.15 mg/L, the nitrate concentrations increased for the remainder of the test from 3.37 to 4.79 mg/L. The sulfate concentrations exhibited increases and decreases in concentration, between 309 and 335 mg/L, for the duration of the pumping test.

The confining aquitard, located at a depth of roughly 9.1 to 14.6 m, is present across the entire study area. The aquitard layer fluctuates in thickness, ranging from approximately 3.1 to 6.6 m, with no evident spatial pattern for variations in thickness (Butler et al., 2004). The hydraulic conductivity of the confining unit has been estimated to be $1.6 \times 10^{-3}$ m/d (Butler et al., 2011). Two observation wells were installed in the aquitard for water-level measurements and sample collection (Table 1).

The HPA, characterized by Quaternary sands with some clay lenses in the upper portion of the aquifer, ranges in thickness from roughly 3.0 to 6.8 m and thins towards the eastern edge of the research site (Butler et al., 2004; Whittemore et al., 2012). Groundwater withdrawal for irrigation from the HPA, in the proximity of the LRS, occurs during the growing season between March and October (Butler et al., 2011). In general, groundwater levels approach recovery after the irrigation season by December (Butler et al., 2011). An additional pumping test determined the transmissivity and storage coefficient of the HPA at this site to be 501 $m^2$/d and $1.7 \times 10^{-4}$, respectively (Butler et al., 2004).

During the HPA pumping test, Butler et al. (2004) collected and analyzed groundwater samples from nearby observation wells for specific conductivity, pH, total dissolved solids, and major and minor dissolved constituent concentrations. The geochemical data indicated a downward vertical flux of water from the shallow aquifer along the gravel pack of the pumping well through the aquitard. The length of the gravel pack surrounding the pumping well screen extended from the shallow alluvial aquifer to the HPA, short-circuiting the aquifer. Water movement through the gravel pack could explain the hydraulic connection between the two aquifers.

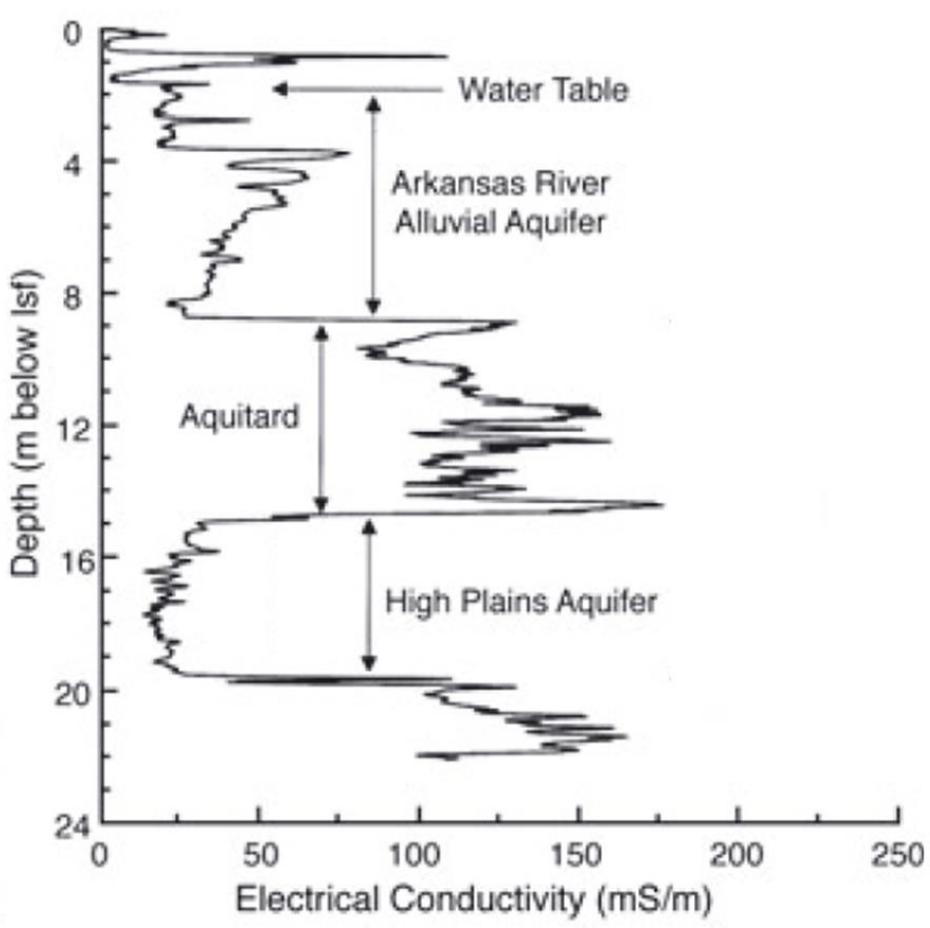


Figure 2. Stratigraphy of the LRS, represented by an electrical conductivity profile (modified from Butler et al., 2011).

The RCS is on a fifth order stream located roughly 110 km to the east of the LRS in Butler County, Kansas (Figure 1). The mean annual precipitation at the site is approximately 850 mm/yr; however, the RCS has been affected by a dry period during the past couple of years. The 32 $km^2$ watershed encompasses 60% pasture, 35% cropland, and 5% woodland (Machavaram et al., 2006). The riparian zone surrounding the river bed usually extends less than 60 m from the stream and contains a variety of vegetation, including oaks, hawthorn, cottonwood, elm, willow, sycamore, and other trees and bushes (Whittemore et al., 2012). Rock Creek was flowing throughout the entire study period of April 2013 to November 2013.

Previous research in the Rock Creek watershed was conducted by Machavaram et al. (2006) to determine the components of stream flow during precipitation events. Deuterium and oxygen-18 isotope measurements and chloride and sulfate concentrations were determined in precipitation, stream, pond, groundwater, and soil moisture samples collected pre- and post- two precipitation events in May 2002. The watershed study indicated the contribution of various water sources, including precipitation, runoff, pond water, and bank storage, to the stream flow at different locations along Rock Creek throughout the precipitation events. The utilization of isotope data, particularly deuterium excess (*d*-excess), indicated complex stream flow dynamics. For example, after the first storm event, the upstream stream flow was primarily composed of shallow groundwater and pond outflow. In contrast, the downstream stream flow components included shallow groundwater flow and surface runoff.

The RCS stream valley includes differing sediment and bedrock layers on each side of the channel (Figure 3). The steep south bank of the river channel is composed of the Permian Holmesville Shale Member of the Doyle Shale with intermittent limestone (University of Colorado and Kansas Geological Survey, 2013). The north bank of the river channel is characterized by several different strata. The overlying soil, ranging in thickness from 1.0 to 2.0 m, is composed of a silty clay loam (Machavaram et al., 2006; University of Colorado and Kansas Geological Survey, 2013). A fine-grained silty clay alluvium subsoil extends from the base of the overlying surface soil downwards to roughly 3.3 m in depth (Figure 3) (Machavaram et al., 2006; Whittemore et al., 2012). Some limestone gravel zones are embedded in the lower part of this layer. The water-table and several observation well screens are located in the lower part of this layer (Figure 3, Table 2). Beneath the subsoil lies a silty-clay layer embedded with gravel, extending from approximately 3.3 to 6.0 m in depth below the land surface. Observation

wells are screened at the base of this clay layer and the top several centimeters of the weathered top of the underlying limestone; these wells are termed the alluvium base wells (Table 2). Permian dolomite and limestone bedrock begins roughly 6.0 m below the land surface (varies between 5.5 and 7.6 m below the land surface across the study area) and includes cavities developed by the dissolution of gypsum-filled fractures, thin beds of gypsum, and carbonate rock (Machavaram et al., 2006; University of Colorado and Kansas Geological Survey, 2013). The alluvium base wells derive most of their water during sampling from the top of the weathered bedrock that was penetrated during the installation of the wells using direct-push technology (Geoprobe). A single bedrock well was drilled to a depth of 11.2 m and encountered a few void spaces probably partially filled with sediment (Table 2).

Several direct-push electrical conductivity logs of unconsolidated sediment have been completed at the RCS (Figure 4) (University of Colorado and Kansas Geological Survey, 2013). The upper portion of the logs generally exhibited low electrical conductivity values with sharp increases at a depth of roughly 2.1 to 3.0 m. The higher electrical conductivity values represent the silty-clay layer. The lower portion of the electrical conductivity logs decreased with depth near the weathered bedrock; the decreasing electrical conductivity may be related to an increasing amount of limestone gravel in the silty-clay. The top of the bedrock is correlated to a zone of low electrical conductivity and high permeability (University of Colorado and Kansas Geological Survey, 2013).

The geochemistry of the surface water and groundwater is governed by groundwater-rock interactions, evapotranspiration, and brine disposal from an oil field (Machavaram et al., 2006). Groundwater-rock interactions include the dissolution of carbonate minerals and cation exchange via clays in the subsurface. Gypsum dissolution results in elevated calcium and sulfate

concentrations in the groundwater (Machavaram et al., 2006). Evapotranspiration, controlled by the riparian vegetation density and climatic conditions, can cause variations in the groundwater levels; an increase in water-level dilutes dissolved ion concentrations, while a decrease in water-level concentrates the ions. A small oil field was commissioned from the 1940s to 1950s near the lower portion of the Rock Creek watershed (Machavaram et al., 2006). An increase in groundwater sodium and chloride concentrations at the RCS is a result of brine disposal from the oil field.

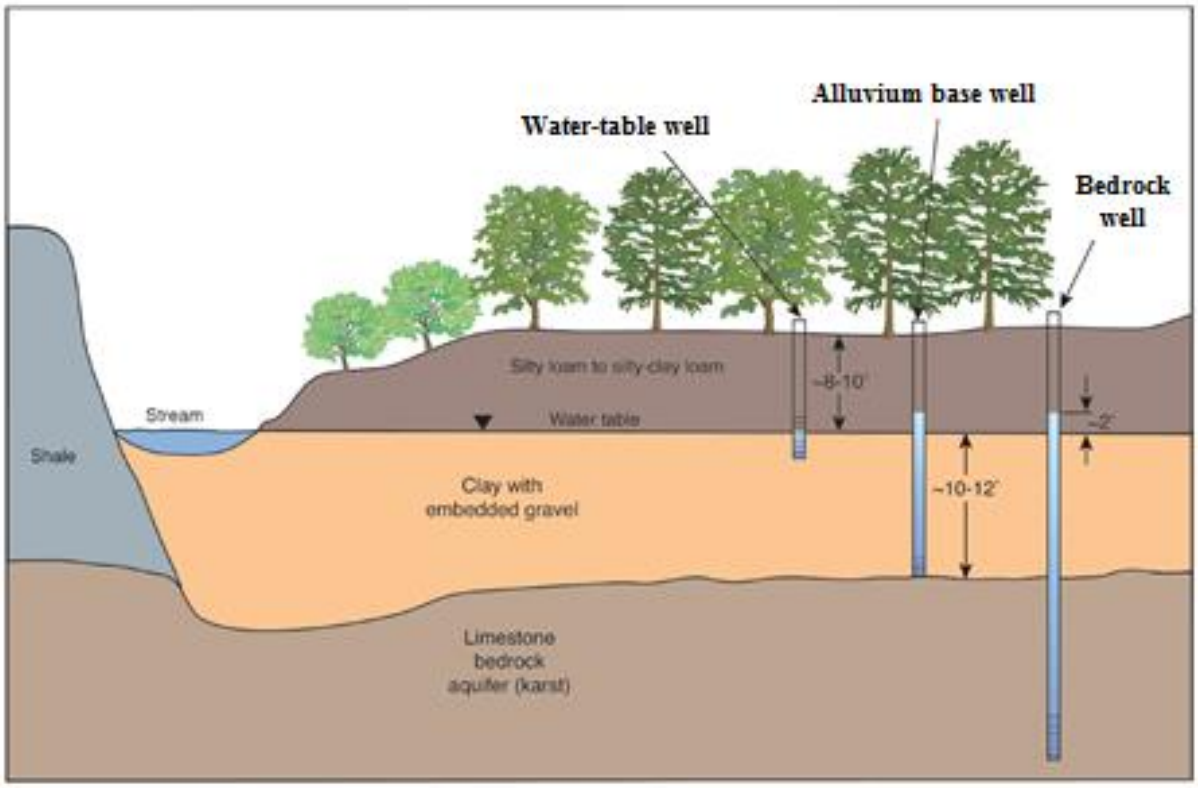


Figure 3. Generalized stratigraphy of the RCS (not to scale) (modified from University of Colorado and Kansas Geological Survey, 2013).

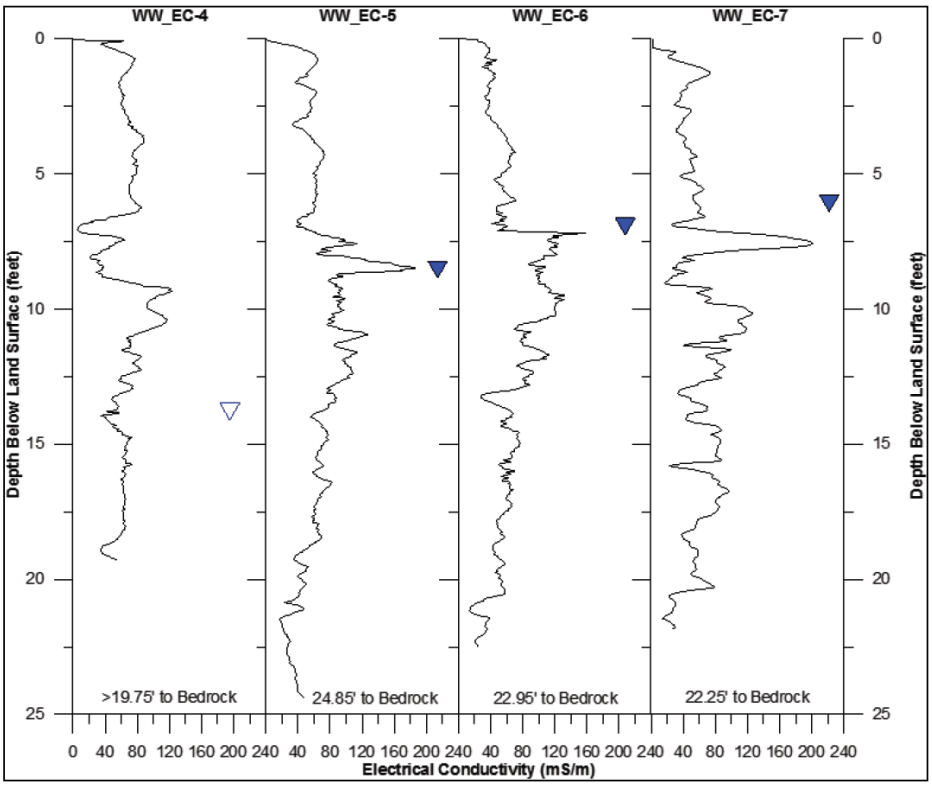


Figure 4. Direct-push electrical conductivity logs of sediment at the RCS. The location of the well logs, WW_EC4-7, correspond to the approximate location of water-table wells D-A, respectively. The filled blue triangles indicate the water level, and the open triangle represents the last water-level measurement before the direct-push hole was sealed (from University of Colorado and Kansas Geological Survey, 2013).

## Methods

Groundwater observation wells were previously installed by the Kansas Geological Survey within the riparian zones surrounding the LRS and RCS using direct-push technology (Geoprobe) as well as hand auger, mud rotary, and sonic well-drilling equipment (Figures 5-6). A time series of surface and groundwater samples were collected from these wells to distinguish variations in groundwater flow pathways. Continuous water-level measurements were recorded by MiniTroll and LevelTroll pressure transducers positioned in almost all wells at both the LRS and RCS.

LRS groundwater samples were collected from the shallow and deep aquifers and clay aquitard (Figure 5, Table 1, Appendix I). Sampling occurred June 7 and July 11, 2013 to observe conditions during the growing season, while November 19, 2012 and October 15, 2013 samples observed the non-growing season. Surface water samples could not be collected during the sampling periods due to the lack of flow in the Arkansas River (Appendix I). Additionally, aquitard water samples were not collected during the growing season due to the slow recovery of the aquitard wells.

Surface and groundwater samples at the RCS were collected on June 13 and September 2, 2013 to observe trends in the growing season, while April 16 and November 7, 2013 samples characterize the non-growing season (Figure 6, Table 2, Appendix I). Stage height data from Rock Creek was collected via pressure transducers upstream and downstream of the groundwater sampling location as well as by an observation well in the streambed.

Daily precipitation accumulation data for the LRS was available from a nearby weather station in Radium, Kansas (Kansas State University, 2014), whereas precipitation data for RCS was collected on location. Previous isotope data for precipitation collected in May 2002, by Marchavarm et al. (2006), was utilized at the RCS. Relative annual and monthly average precipitation isotope compositions at both sites were determined by the Online Isotopes Precipitation Calculator (Bowen and Revenaugh, 2003; Bowen et al., 2005; OIPC, 2014).

Figure 5. Groundwater well locations at the LRS (modified from Google Earth, "Larned," 2014).

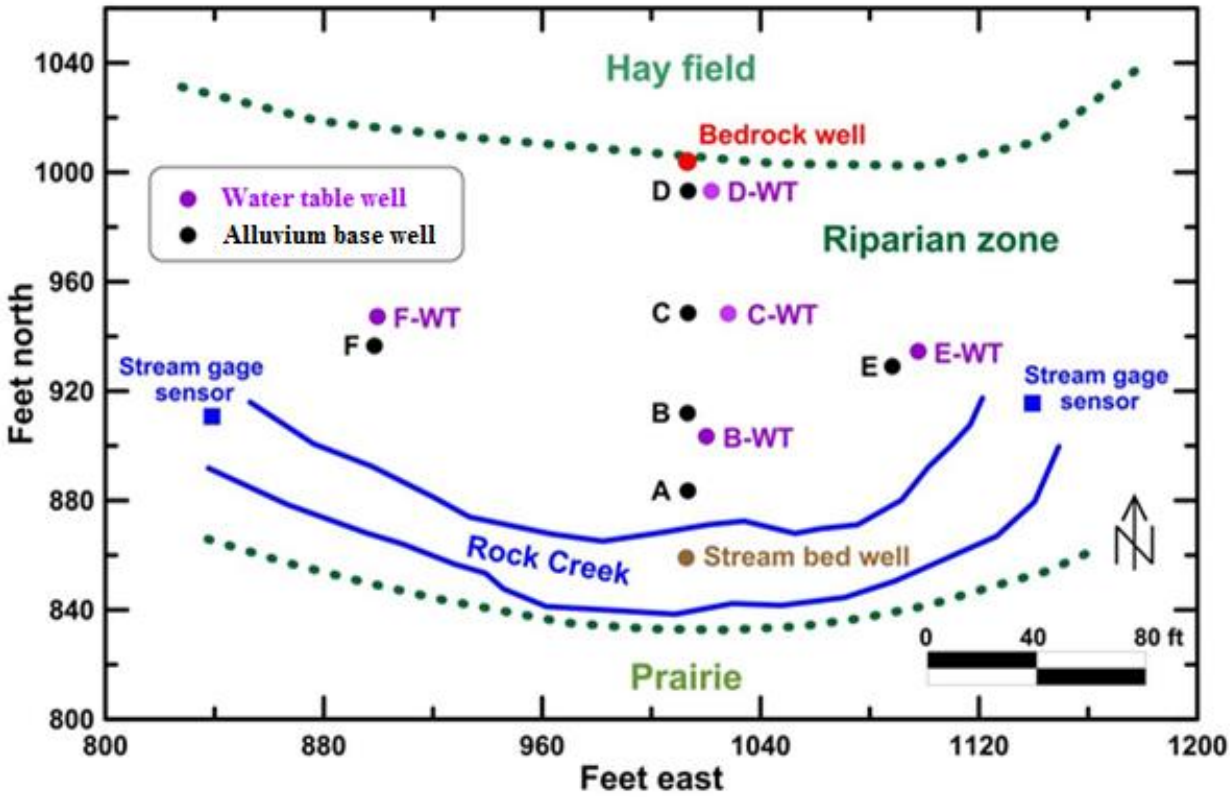

Figure 6. Groundwater well locations at the RCS (from Whittemore et al., 2012).

Table 1. The LRS well characteristics.

| Well ID | Screen Interval Below Land Surface (m) | Average Screen Depth Below Land Surface (m) | Screen Location |
|---|---|---|---|
| LWPH6 | 0.65-2.86 | 1.75 | Shallow Aquifer |
| LWPH3 | 0.76-2.96 | 1.86 | Shallow Aquifer |
| LWPH4A | 0.80-3.00 | 1.90 | Shallow Aquifer |
| LWPH2 | 0.95-3.12 | 2.03 | Shallow Aquifer |
| LWPH4B | 7.03-8.38 | 7.71 | Shallow Aquifer |
| LWCB1 | 10.12-10.73 | 10.43 | Aquitard |
| LWCB2 | 11.64-12.25 | 11.95 | Aquitard |
| LWPH4C | 16.64-17.98 | 17.31 | HPA |

Table 2. The RCS well characteristics.

| Well ID | Screen Interval Below Land Surface (m) | Average Screen Depth Below Land Surface (m) | Screen Location |
|---|---|---|---|
| B-WT | 2.29 - 3.05 | 2.67 | Water Table |
| C-WT | 3.14 - 3.23 | 3.19 | Water Table |
| D-WT | 3.05 - 3.81 | 3.43 | Water Table |
| E-WT | 3.26 - 4.03 | 3.65 | Water Table |
| F-WT | 3.15 - 3.91 | 3.53 | Water Table |
| Well A | 5.28 - 5.99 | 5.64 | Alluvium Base |
| Well B | 5.52 - 6.23 | 5.88 | Alluvium Base |
| Well C | 5.29 - 6.00 | 5.65 | Alluvium Base |
| Well D | 5.81 - 6.52 | 6.17 | Alluvium Base |
| Well E | 5.31 - 6.23 | 5.77 | Alluvium Base |
| Well F | 5.81 - 6.52 | 6.17 | Alluvium Base |
| Well H | 9.72 - 12.65 | 11.19 | Bedrock |

Before sampling, each well was purged using a Geotech Geopump peristaltic pump or a Geotech Geosquirt pump for roughly fifteen to thirty minutes. The conductivity of the pumped water was monitored. Geochemical and isotope samples were collected in 500 mL and 30 mL sample bottles, respectively. Duplicate samples were taken within a one to ten minute period depending on the pumping rate and availability of groundwater at each individual well. At the time of the sample collection, groundwater levels were measured with an electronic tape, and water temperature and specific conductance were measured with a Yellow Springs Instrument meter.

Geochemical and isotope samples were transported on ice and refrigerated until laboratory analyses could be completed. The geochemical analysis was conducted at the Kansas Geological Survey in Lawrence, Kansas. Analysis included filtration through a 0.45 μm membrane filter, determination of lab pH, and alkalinity titration. An inductively coupled plasma optical emission spectrometer was used for the determination of Ca, Mg, Na, K, Sr, B, and silica concentrations, and an ion chromatograph for Cl, $SO_4$, $NO_3$, F, and Br concentrations. The estimated analytical error was generally on the order of a few percent for each constituent. Detection limits are on the order of magnitude relative to the last significant figure reported (Appendix II). Total dissolved solid (TDS) concentrations were computed from summing major and minor dissolved constituents with bicarbonate multiplied by 0.4917 to represent carbonate that would be precipitated. All calculated charge balances were below 3.5%. The deuterium and oxygen-18 isotopic compositions ($\delta^2H$ and $\delta^{18}O$) were analyzed at the Keck Paleoenvironmental Stable Isotope Laboratory at the University of Kansas in Lawrence, Kansas via a L2120-i Picarro Cavity Ring-Down Spectrometer with High-Precision Vaporizer A0211. The isotopic measurements were recorded in δ notation (‰), relative to the international VSMOW standard. The analytical error was <0.5‰ for deuterium and <0.1‰ for oxygen-18. The geochemical and isotopic values for duplicate samples at each individual LRS and RCS well were averaged (Appendix II).

# Chapter 3: Results

## LRS

### Water Level

The water-level and piezometric surface in the LRS wells exhibited varying responses to pumping during the sampling events based on the screen depths of each individual well. The

shallow aquifer wells did not have a significant change in water level during any sampling event (Figure 7). The water level in the aquitard well exhibited an immediate response, dropping 3.16 m, after the groundwater sampling event in November 2012. The water level in the aquitard well did not approach full recovery until late September 2013 and dropped 4.37 m in response to the groundwater sampling event in October 2013. The piezometric surface of the HPA well dropped 0.9 m after the October 2013 sampling event and had several sharp drops in late June, early August, and early and mid-September 2013.

Precipitation events of varying accumulation totals had diverse effects on the well water levels in each subsurface unit. The largest single day precipitation event (totaling 53.85 mm) occurred May 30, 2013. Water levels in all shallow aquifer wells increased roughly 0.04 m immediately following the precipitation event (Figure 7). In contrast, the water level in aquitard well did not exhibit an immediate, significant change. The HPA well experienced a slight rise, followed by a sharp decrease in water level. Another large multiday precipitation event occurred August 2-5 and August 8-9 (totaling 94.74 mm). The water levels in the shallow aquifer well increased 0.87 m by August 17, a couple days after the precipitation event. The water level in the aquitard well exhibited a slight increased rate of recovery at the same time as the shallow aquifer. In contrast, the water level in the HPA well experienced multiple sharp drops and rises in water level that are expected to have been caused by irrigation pumping. Irrigation pumping in the HPA did not affect the water levels of the alluvial aquifer wells.

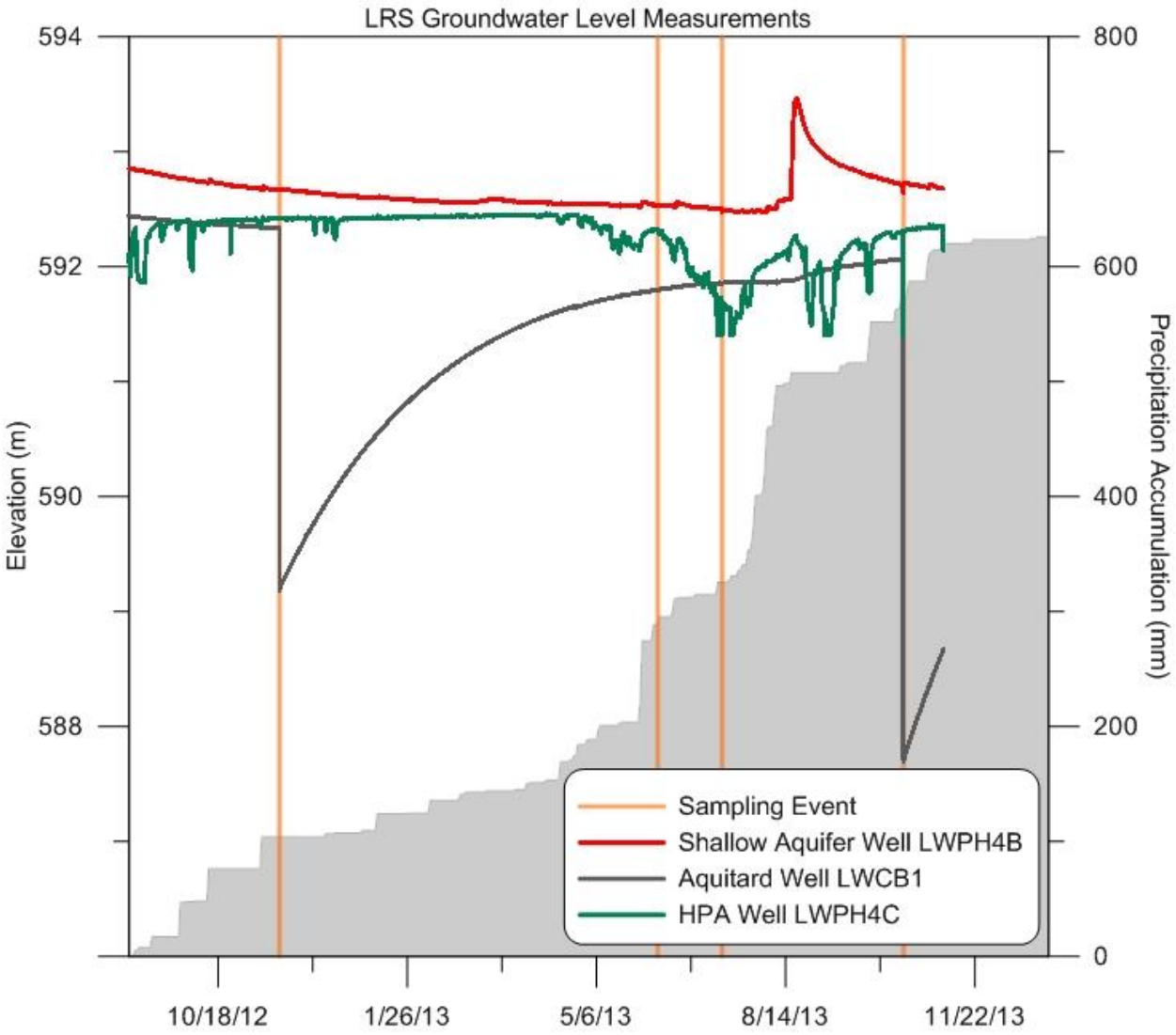


Figure 7. Water levels of the shallow and deep aquifers and aquitard at the LRS. Precipitation data, represented by the shaded gray area, is a cumulative total of daily accumulation. The water-level measurements were recorded every fifteen minutes. Elevations of the LRS wells have been surveyed; the units are meters above mean sea level (AMSL).

**Geochemical Analysis**

The continuous conductivity measurements recorded in the shallow aquifer well LWPH4A decreased in direct response to the multi-day precipitation event in August (Figure 8, Appendix I). After the precipitation event, the water level in the well rose while the conductivity quickly decreased and proceeded to rise and fall in the following month.

Dissolved solid concentrations in the shallow aquifer wells exhibited seasonal variability, while the aquitard and HPA well concentrations remained relatively constant. At each sampled shallow aquifer well, TDS and sulfate concentrations were lower in the non-growing season compared to the growing season (Figures 9 and 11). Nitrate concentrations were essentially the same in both seasons, except for the lower concentrations observed in the shallow aquifer wells LWPH2 and LWPH4A during the October 2013 sampling event (Figure 10). In the same sampling event, a decrease in TDS, nitrate, and sulfate concentrations was observed in wells LWPH2 and LWPH4A relative to the other sampling events (Figures 9-11). Water from the aquitard well consistently had the lowest dissolved solid concentrations compared to water from both aquifers (Figures 9-11, Appendix II). The HPA well concentrations remained relatively constant for each sampled dissolved constituent.

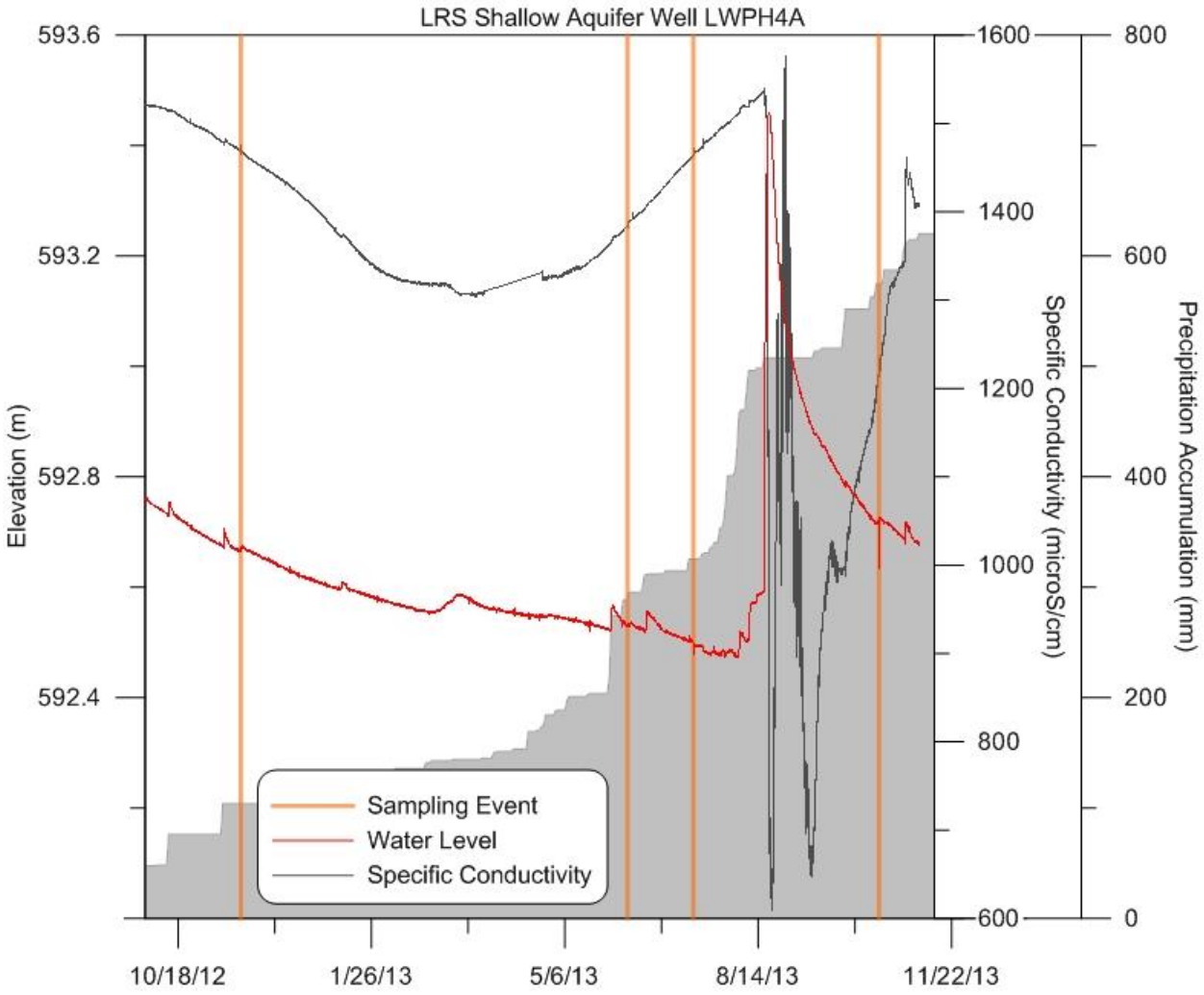


Figure 8. Groundwater elevations and corresponding specific conductivity for the LRS shallow aquifer well LWPH4A. Precipitation data, represented by the shaded gray area, is a cumulative total of daily accumulation. The water levels were recorded every fifteen minutes. Well elevations have been surveyed; the units are meters AMSL.

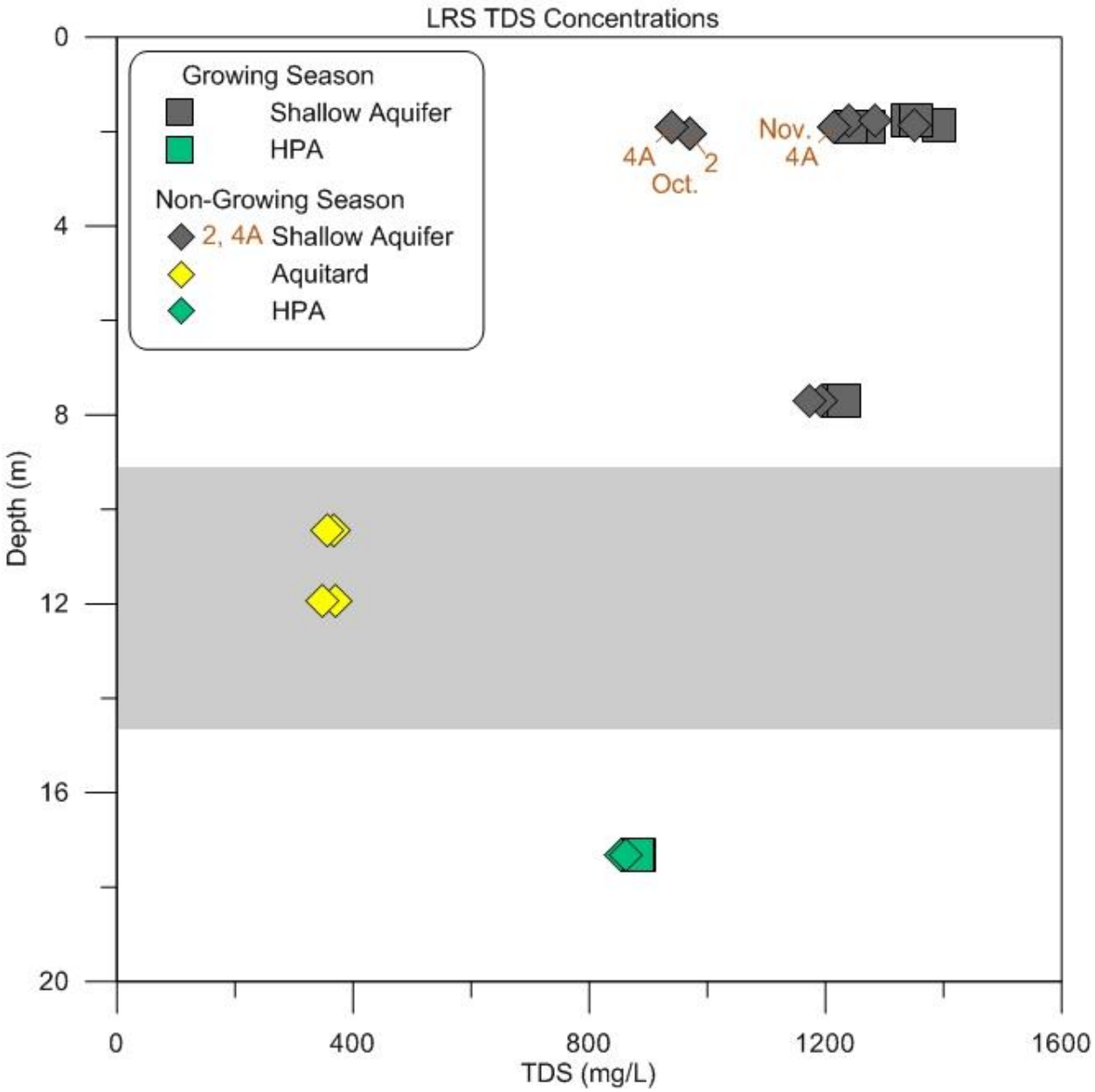


Figure 9. TDS concentrations vs. average well screen depth at the LRS. The shaded gray area represents the approximate location of the aquitard (aquitard thickness varies from 3.1 to 6.6 m across the study area).

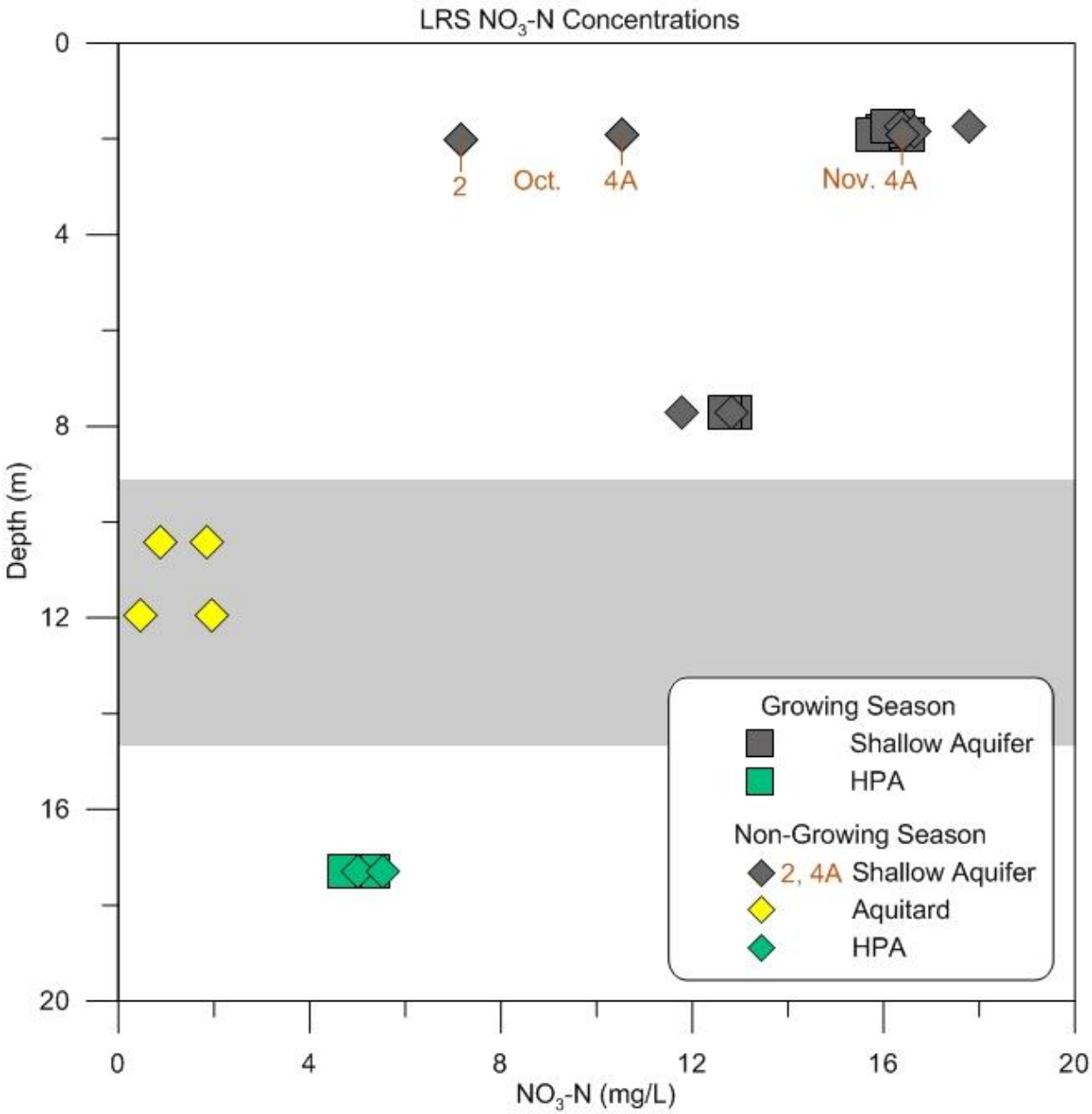


Figure 10. Nitrate concentrations vs. average well screen depth at the LRS. The shaded gray area represents the approximate location of the aquitard (aquitard thickness varies from 3.1 to 6.6 m across the study area).

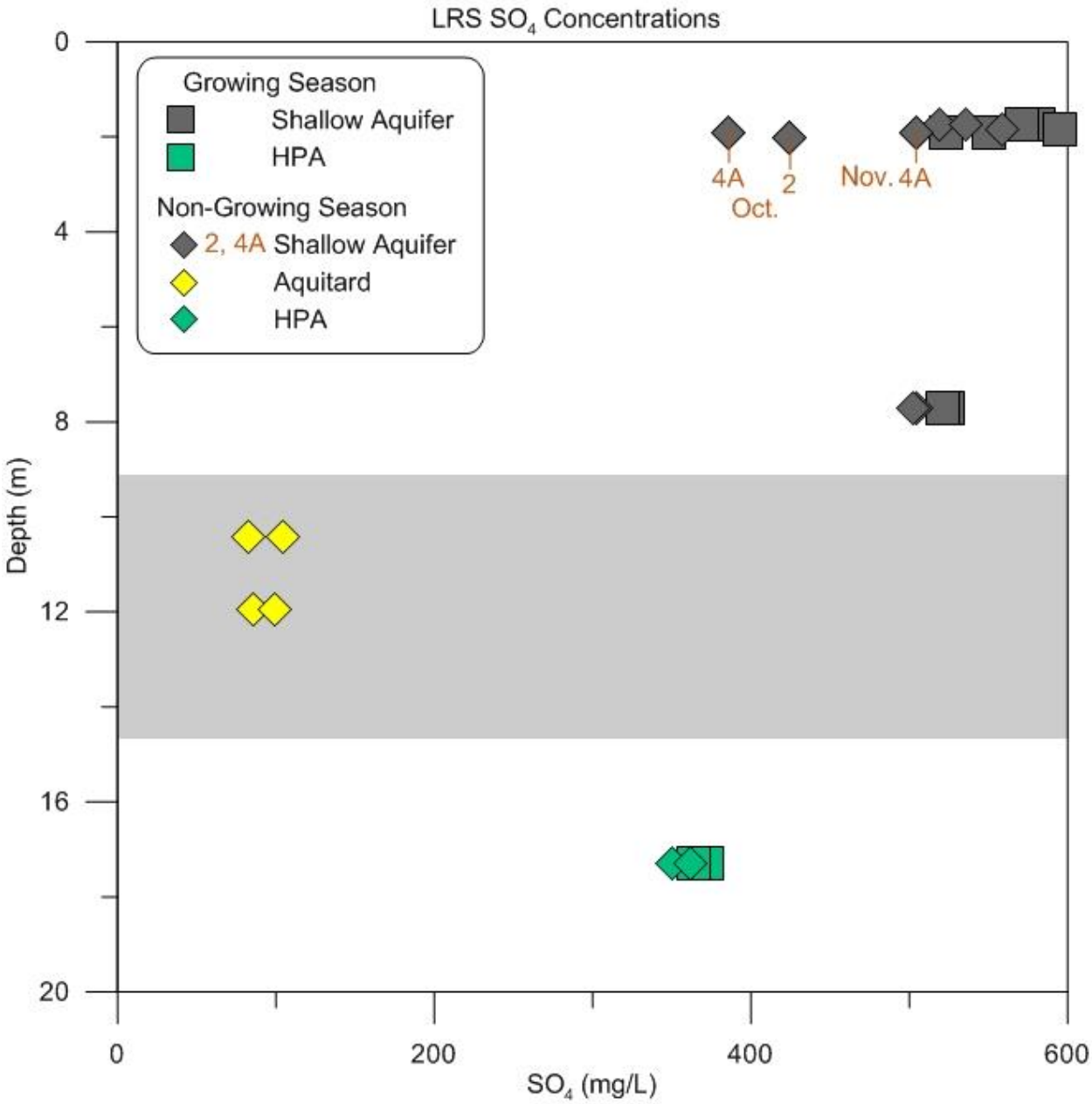


Figure 11. Sulfate concentrations vs. average well screen depth at the LRS. The shaded gray area represents the approximate location of the aquitard (aquitard thickness varies from 3.1 to 6.6 m across the study area).

**Isotopic Analysis**

The stable isotope compositions became lighter with depth from the shallow to the deep aquifer wells, whereas the aquitard wells exhibited the lightest isotopic compositions (Figure 12,

Appendix II). During the growing and non-growing seasons, the isotopic compositions of the shallow aquifer wells were above the global meteoric water line (GMWL). The shallow aquifer well samples exhibited a larger isotopic range during the non-growing season compared to the growing season (Table 3a-b). Two shallow aquifer wells, LWPH2 and LWPH4A, exhibited significantly heavier isotope compositions in the October sampling event compared to all the other shallow aquifer well samples. Well LWPH4B, the deepest shallow aquifer well and closest in vertical depth to the aquitard, exhibited the lightest isotopic compositions among the shallow aquifer wells in both seasons. The isotopic compositions of the aquitard well samples were below the GMWL during both seasons. The aquitard samples had the most depleted isotopic compositions of all the LRS groundwater samples by 16‰ for deuterium and 1.4‰ for oxygen-18. The isotopic compositions of the HPA well samples were located above the GMWL and were similar for both seasons (Table 3a-b). During the non-growing season, all groundwater samples collected at the LRS were isotopically lighter in November 2012 compared to October 2013.

Seasonal variations of precipitation isotopic compositions were calculated for the LRS (Figure 12). The summer precipitation exhibited the heaviest isotopic composition and was located below the GMWL. This value was closer to the isotopic compositions of the shallow aquifer and HPA wells than to the values of the aquitard. The isotopic compositions of the aquitard well were located between the annual, spring, and fall average precipitation values.

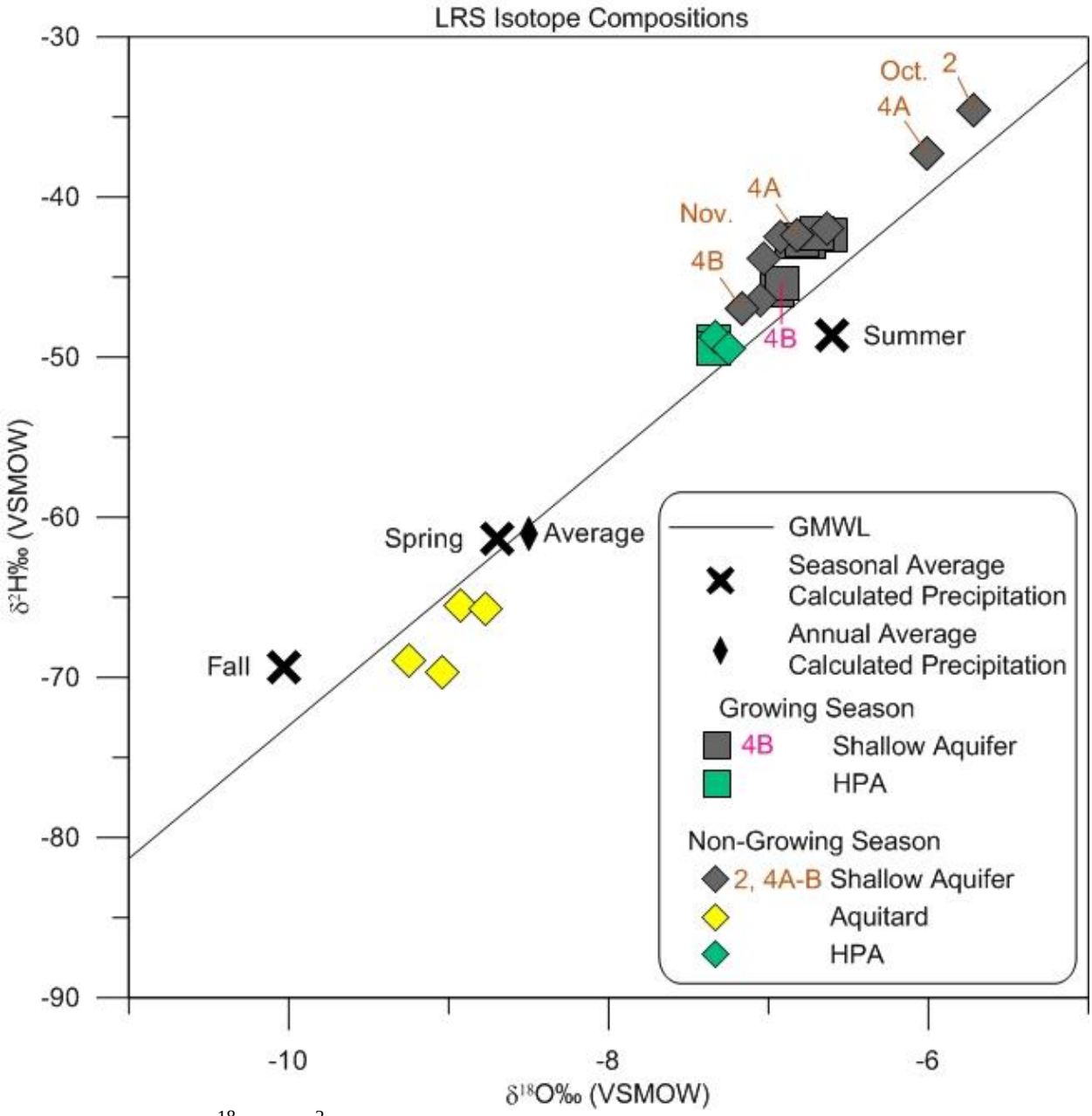


Figure 12. Plot of $\delta^{18}O$ vs. $\delta^{2}H$ measurements from all sampling events at the LRS. Relative seasonal and annual average calculated precipitation isotope compositions were determined by the Online Isotopes Precipitation Calculator (Bowen and Revenaugh, 2003; Bowen et al., 2005; OIPC, 2014). The summer months included June, July, and August; the spring months included March, April, and May; and the fall months included September, October, and November.

Table 3. The LRS minimum, maximum, average, and standard deviation of groundwater stable isotope data with n representing the number of collected water samples. a) Growing season. b) Non-growing season.

a. Growing Season

| Groundwater Subdivision | Minimum ‰ (VSMOW) | | Maximum ‰ (VSMOW) | | Average ‰ (VSMOW) | | Standard Deviation ‰ (VSMOW) | |
|---|---|---|---|---|---|---|---|---|
| | $\delta^2H$ | $\delta^{18}O$ | $\delta^2H$ | $\delta^{18}O$ | $\delta^2H$ | $\delta^{18}O$ | $\delta^2H$ | $\delta^{18}O$ |
| Shallow Aquifer (n=7) | -46 | -7.0 | -42 | -6.6 | -43 | -6.8 | 1 | 0.1 |
| HPA (n=2) | -49 | -7.4 | -49 | -7.3 | -49 | -7.3 | 0 | 0.0 |

b. Non-Growing Season

| Groundwater Subdivision | Minimum ‰ (VSMOW) | | Maximum ‰ (VSMOW) | | Average ‰ (VSMOW) | | Standard Deviation ‰ (VSMOW) | |
|---|---|---|---|---|---|---|---|---|
| | $\delta^2H$ | $\delta^{18}O$ | $\delta^2H$ | $\delta^{18}O$ | $\delta^2H$ | $\delta^{18}O$ | $\delta^2H$ | $\delta^{18}O$ |
| Shallow Aquifer (n=8) | -47 | -7.2 | -34 | -5.7 | -41 | -6.6 | 4 | 0.5 |
| Aquitard (n=4) | -70 | -9.3 | -65 | -8.7 | -67 | -9.0 | 2 | 0.2 |
| HPA (n=2) | -49 | -7.3 | -49 | -7.2 | -49 | -7.3 | 0 | 0.1 |

## RCS

### Water Level

Two multi-day precipitation events at the RCS, one on May 29-30 (totaling 37.4 mm) and another August 4-9 (totaling 97 mm), exhibited different effects on the stream stage height (Figure 13). The stream stage height increased within days of each precipitation event before returning to base flow. The stream stage increased 0.83 m within a day of the May precipitation event and returned to base flow six days later. The August precipitation event caused an increase of 2.4 m on August 6, and the stream stage returned to base flow on August 15.

Each water-table well responded differently to the precipitation events (Figure 14). The water levels in water-table wells B, C, and E had small peaks, less than roughly 0.35 m, within a

day of the May precipitation event. During the August precipitation event, the water-table well water levels rose between 0.9 and 1.2 m. The exception was the water level in water-table well F, which remained at a constant low level, 300.3 m, except for two peaks (increase of 0.73 m and 1.86 m) that correspond to the precipitation events. After a certain length of time, dependent on the amount of precipitation, the well water level returned to 300.3 m.

All of the alluvium base wells and the bedrock well exhibited similar water-level trends; the water levels rose as a result of the precipitation events and proceeded to continually rise and drop throughout the entire sampling period. The short-term rises and drops are caused by pumping of two nearby (about a 400 m distance) lawn and garden wells located to the north-northwest of the study site.

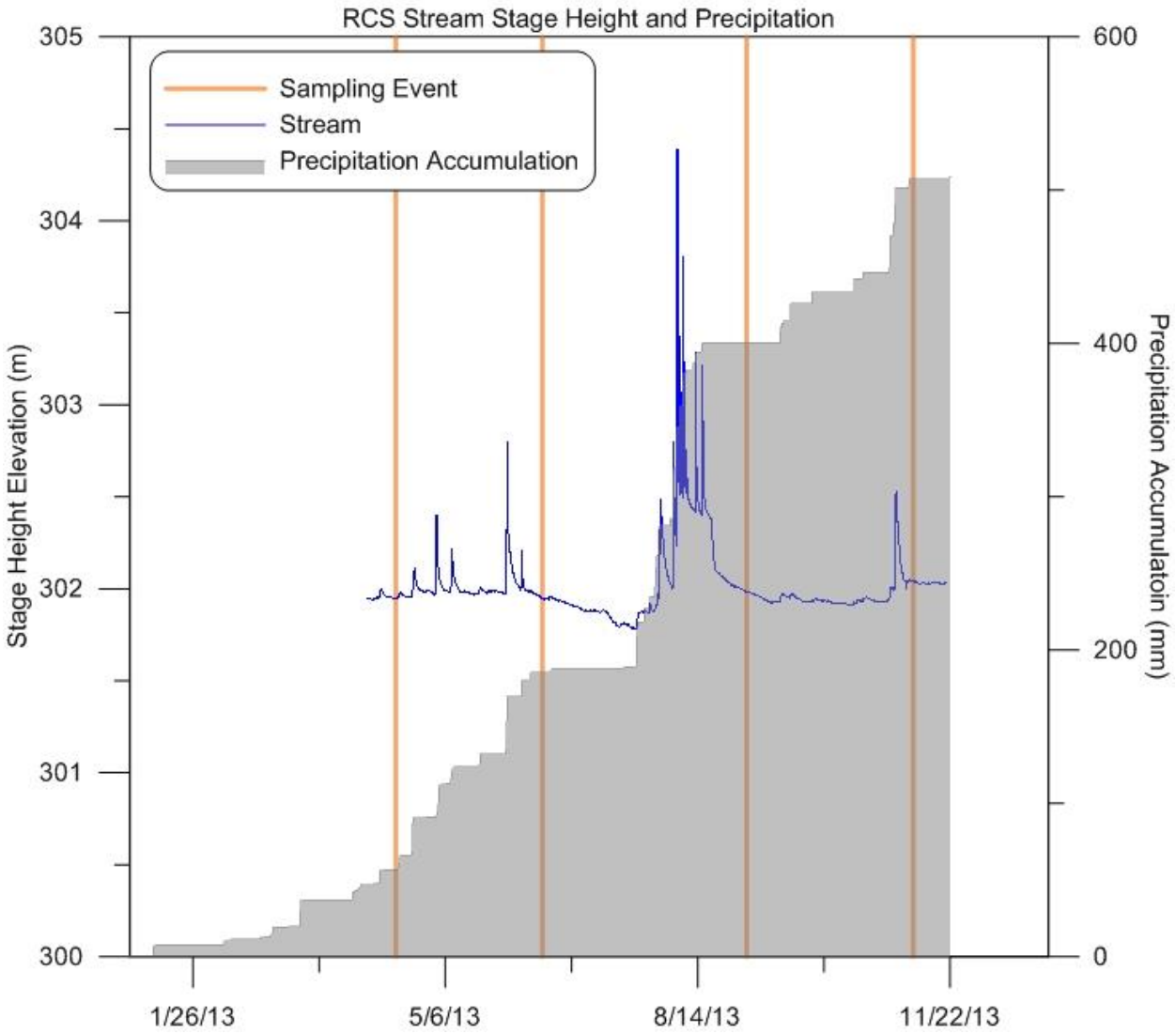

Figure 13. The stage height measurements of Rock Creek were recorded upstream of the groundwater sampling location. Precipitation data, represented by the shaded gray area, is a cumulative total of data collected every fifteen minutes. Stage height measurements are set at a base level of about 302 m for display on the graph.

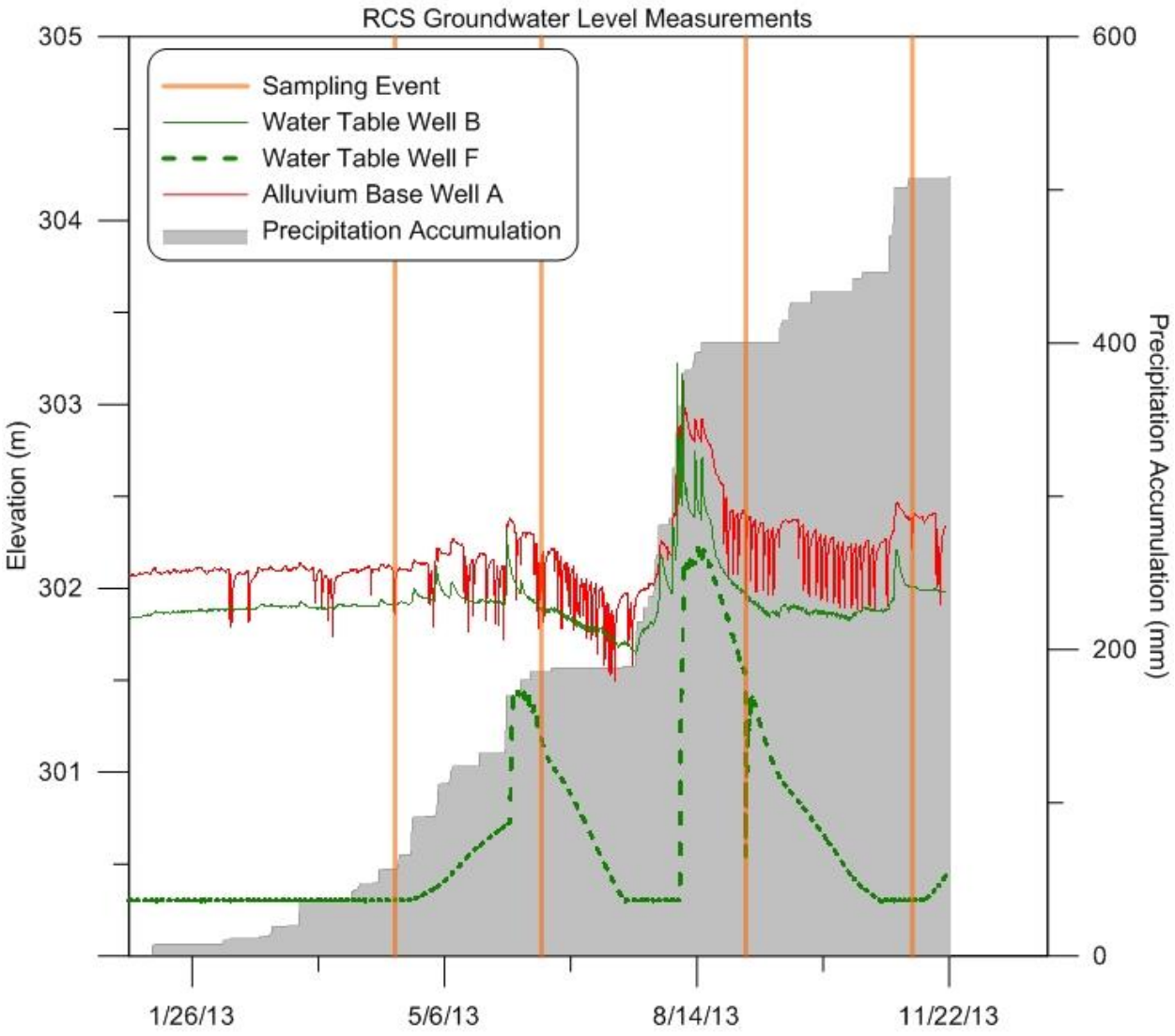


Figure 14. Water levels of the water-table wells and an alluvium base well at the RCS compared to precipitation measurements. Precipitation data, represented by the shaded gray area, is a cumulative total of data collected every fifteen minutes. Water levels were recorded every fifteen minutes. Water-level measurements are relative to each other and a datum of 302 m for display on the graph.

**Geochemical Analysis**

Dissolved solid concentrations varied with location and screen interval depth beneath the land surface. Specifically, the stream and water-table well samples varied between sampling events, while the alluvium base and bedrock samples exhibited roughly consistent constituent concentrations during both seasons (Figures 15-17, Appendix II). Stream TDS, nitrate, and

sulfate concentrations decreased as the year progressed, which resulted in wider concentration ranges between the two non-growing season sampling events compared to the two growing season sampling events (Figures 15-17).

The water-table wells exhibited the largest range of dissolved solid concentrations and showed seasonal variations (Figures 15-17). Water-table well B had the largest range of TDS values, 1,310 to 2,130 mg/L, and water-table well F had the highest concentration of 2,200 mg/L in September (Figure 15). Nitrate concentrations in all water-table wells, excluding water-table well D, were low (<0.5 mg/L) (Figure 16). Water-table well D nitrate concentrations changed with each sampling event, ranging from 1.09 mg/L in November to 2.24 mg/L in April. The April samples from water-table wells B and C had the highest sulfate concentration, 513 and 538 mg/L, respectively, compared to all other water-table samples (Figure 17).

TDS values in the alluvium base wells were slightly lower at all locations in June compared to September (Figure 15). The nitrate and sulfate concentrations of the alluvium base wells varied only slightly between the sampling seasons (Figures 16-17).

The bedrock water samples had very similar concentrations of dissolved solids and all constituents between each season (Figures 15-17).

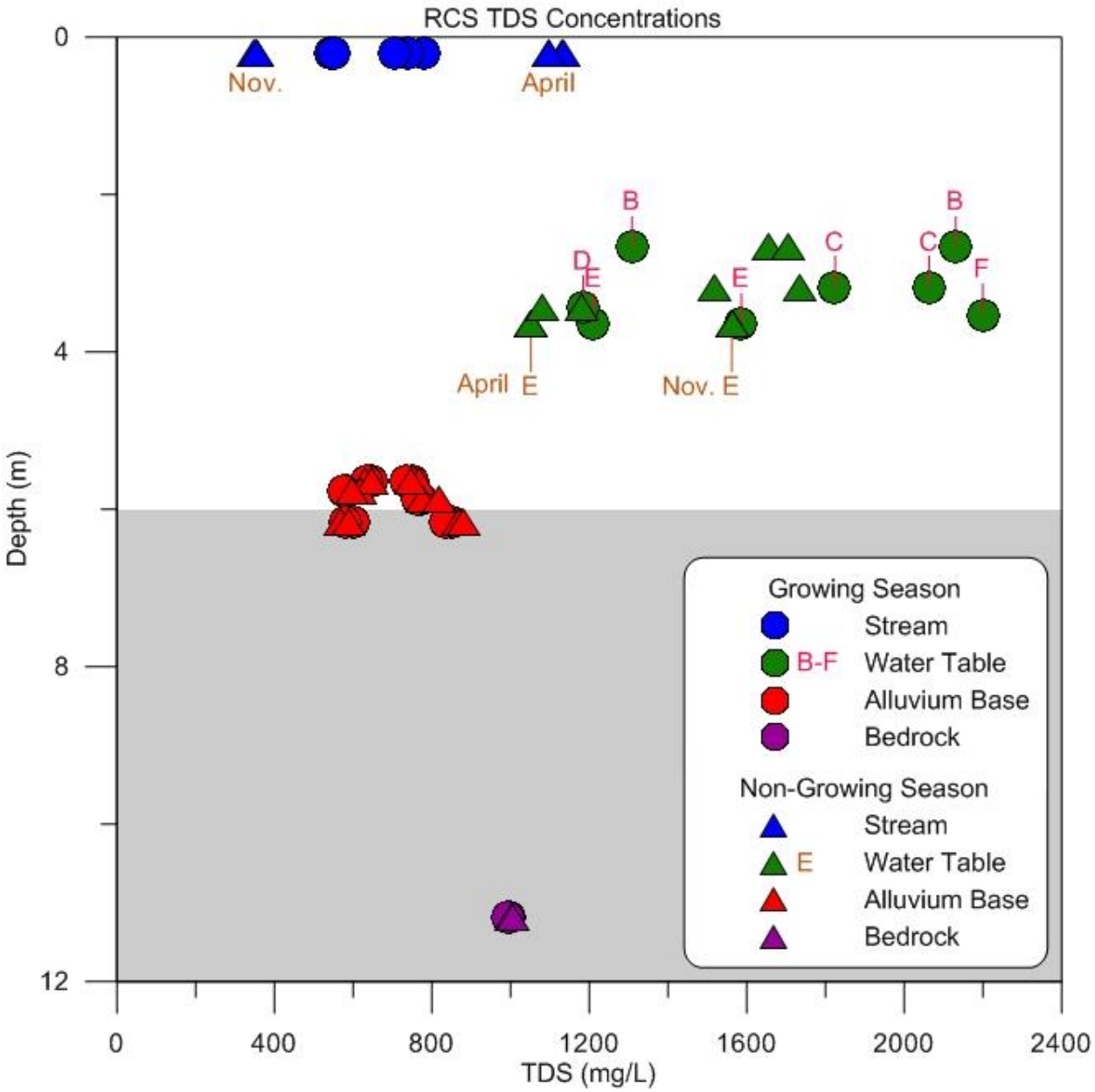


Figure 15. TDS concentrations vs. average well screen depth at the RCS. The shaded gray area represents the approximate location of the bedrock (depth to the bedrock varies between 5.5 and 7.6 m below the land surface across the study area). Stream samples are located at a depth of 0.2 m for clarity.

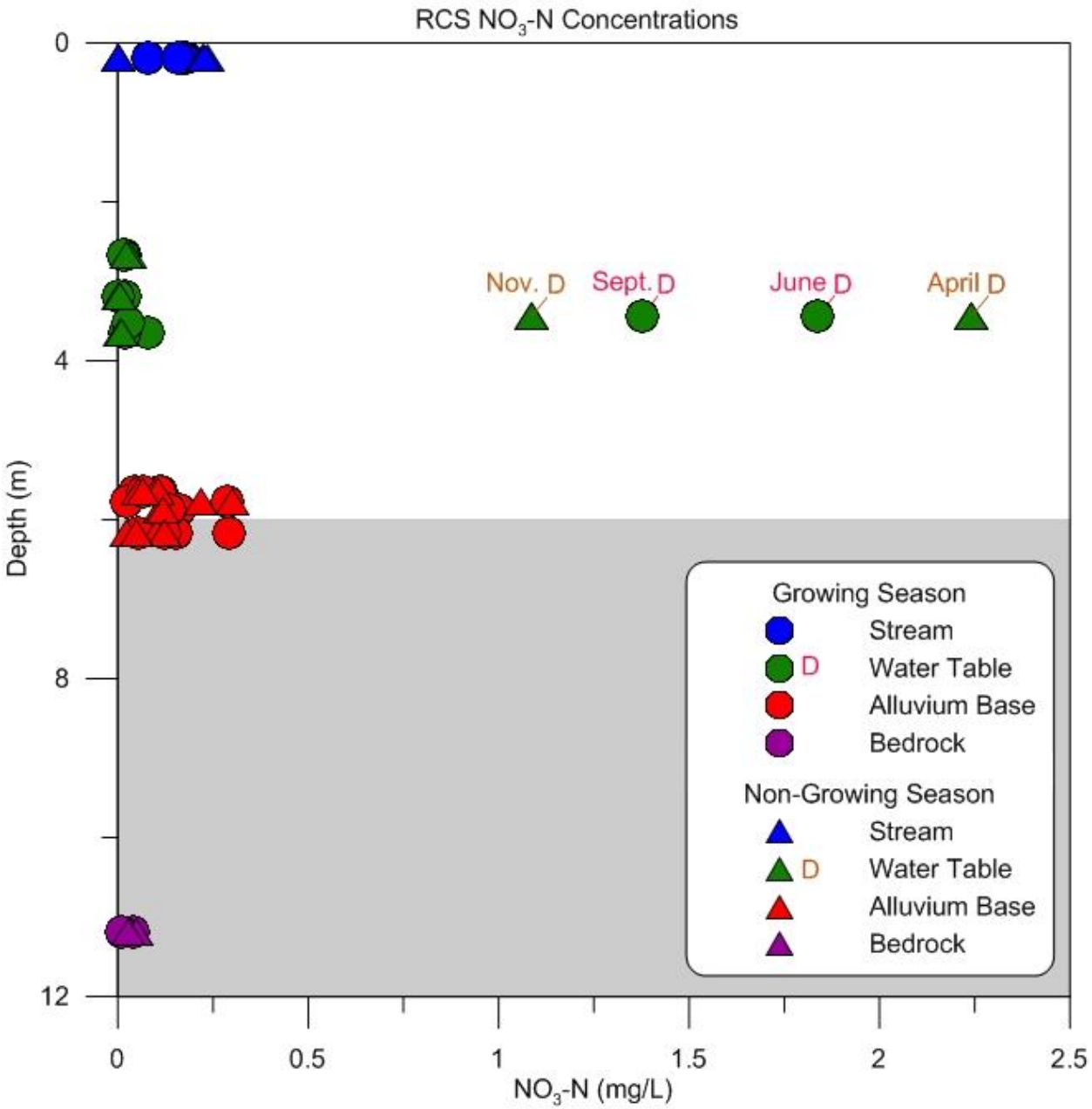


Figure 16. Nitrate concentrations vs. average well screen depth at the RCS. The shaded gray area represents the approximate location of the bedrock (depth to the bedrock varies between 5.5 and 7.6 m below the land surface across the study area). Stream samples are located at a depth of 0.2 m for clarity.

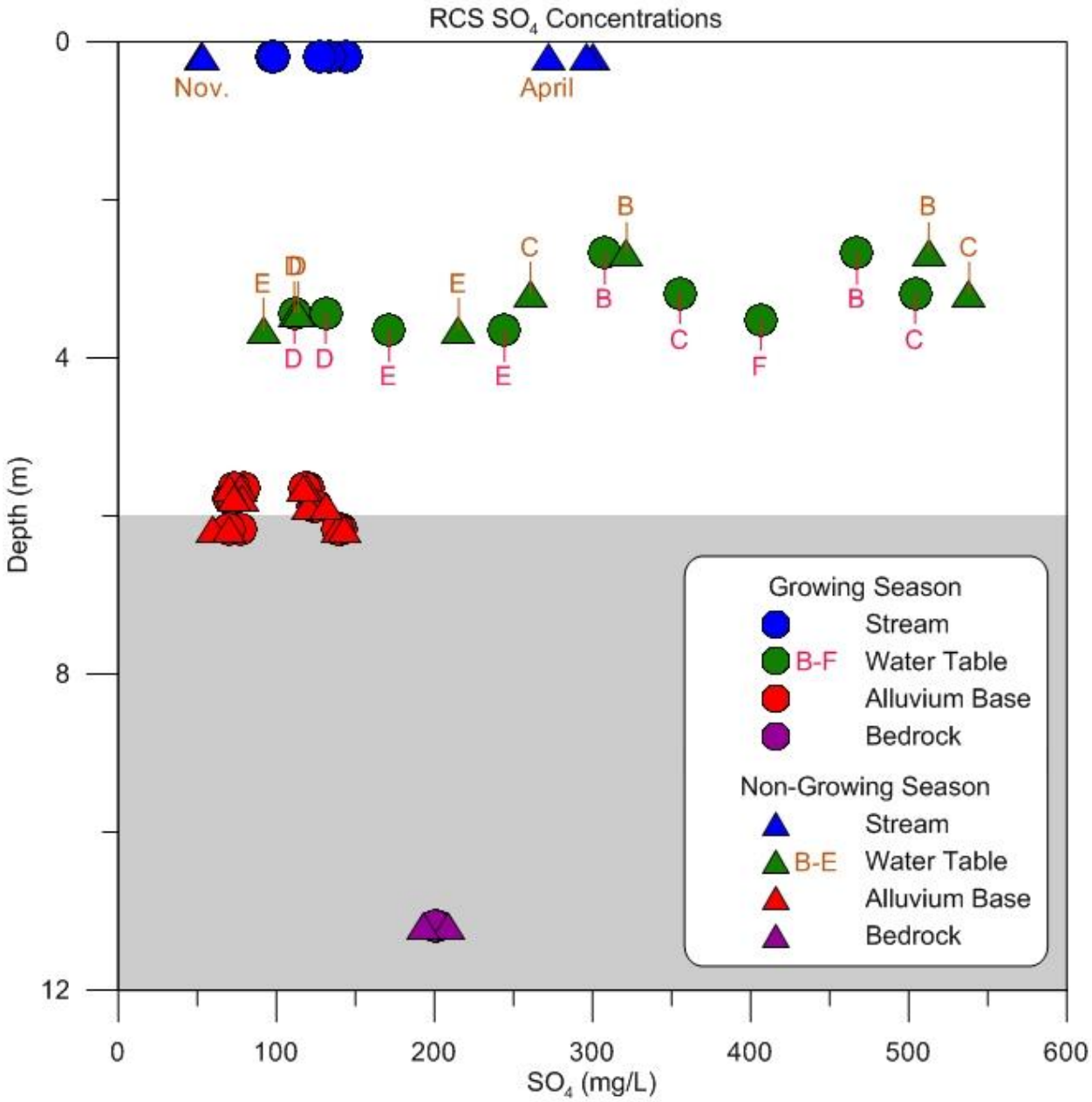


Figure 17. Sulfate concentrations vs. average well screen depth at the RCS. The shaded gray area represents the approximate location of the bedrock (depth to the bedrock varies between 5.5 and 7.6 m below the land surface across the study area). Stream samples are located at a depth of 0.2 m for clarity.

**Isotopic Analysis**

The stream and water-table well samples exhibited the heaviest isotopic compositions at the RCS (Figure 18). The stream samples were slightly lighter in deuterium during the non-

growing season compared to the growing season. During the growing season, the September stream samples were lighter in oxygen-18 compared to the June samples, but exhibited similar deuterium compositions. The isotopic compositions of the water-table wells varied above and below the GMWL depending on the sample event (Figure 18). The water-table wells exhibited the largest range of isotopic values during the growing season (Table 4a-b). Compared to all other water-table wells, samples from water-table wells B and C were heavier in isotope composition and closer in composition relative to the stream samples collected in this study and precipitation samples collected by Machavaram et al. (2006).

The similarity of isotopic compositions between the stream and water-table wells B and C samples varied during each sampling event. During the growing season, the June water-table well samples were closer in composition to the June stream samples compared to the September samples. In the non-growing season, deuterium values in the water-table well samples were lighter and nearer to the GMWL in April compared to November.

The alluvium base and bedrock well samples were similar in isotopic compositions and located above the GMWL (Figure 18, Appendix II). Although the alluvium base and bedrock well samples were similar in isotopic values, some of the alluvium base well samples were lighter compared to those from the bedrock well. In the growing season, all June water-table samples were isotopically lighter than the bedrock sample. During the non-growing season, all April alluvium base well samples, excluding well E, were lighter in deuterium compared to the bedrock sample. The average *d*-excess of the alluvium base well samples was 14.2‰, whereas the average for the bedrock well samples was 12.9‰ (Appendix II).

Calculated precipitation isotopic compositions vary seasonally at the RCS (Figure 18). Summer precipitation has the heaviest isotopic composition and is located below the GMWL.

This value resembles the isotopic compositions of the stream and water-table well B and C samples. The spring precipitation isotopic composition was isotopically heavier and similar to the annual average precipitation composition. The isotopic compositions of the alluvium base and bedrock well samples were located between the summer, spring, and annual precipitation values.

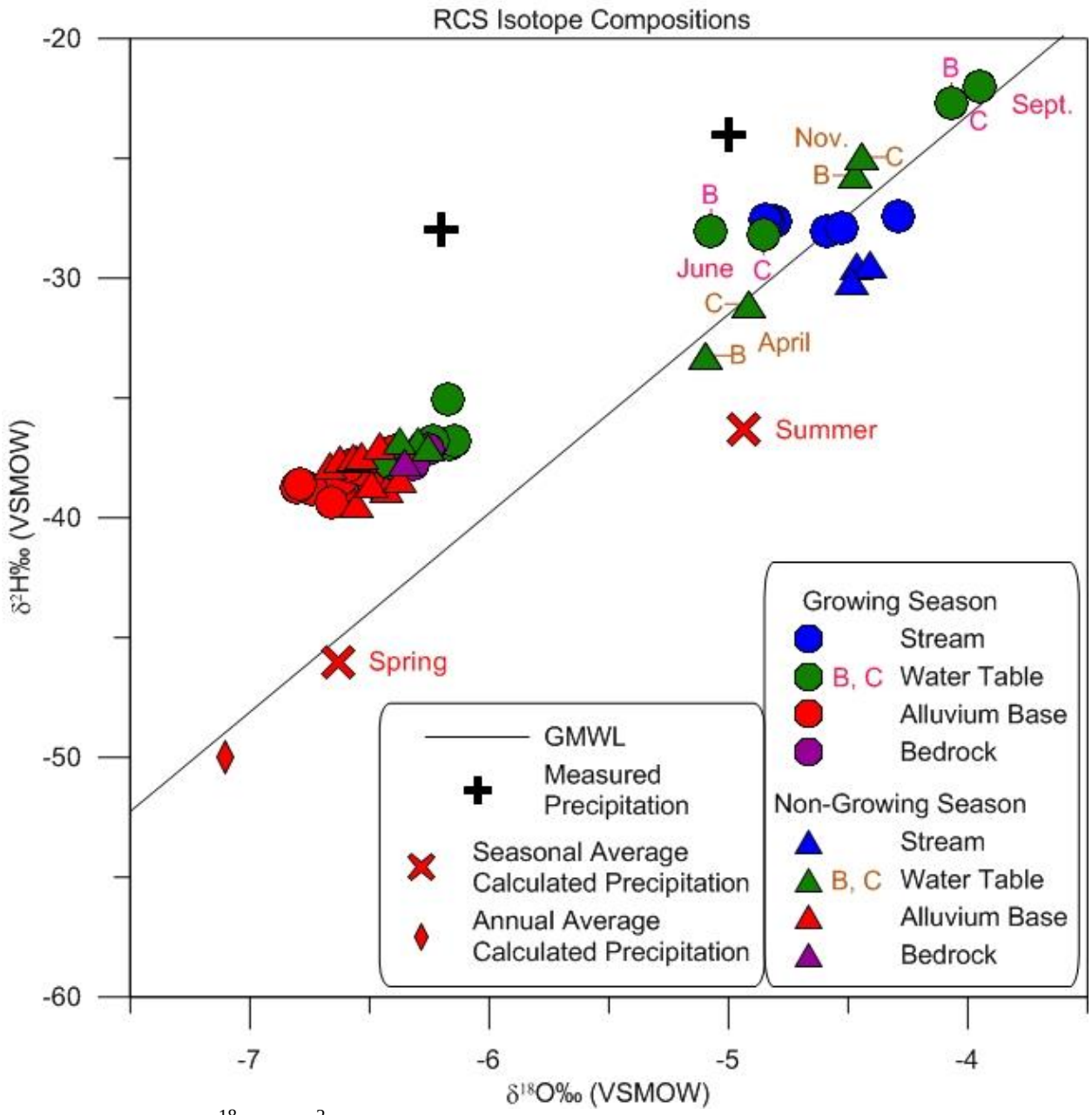


Figure 18. Plot of $\delta^{18}O$ vs. $\delta^{2}H$ measurements from all sampling events at the RCS. The measured precipitation isotope composition data were collected in May 2002 by Machavaram et al. (2006). Relative seasonal and annual average calculated precipitation isotope compositions were determined by the Online Isotopes Precipitation Calculator (Bowen and Revenaugh, 2003; Bowen et al., 2005; OIPC, 2014). The summer months included June, July, and August while the spring months included March, April, and May.

Table 4. The RCS minimum, maximum, average, and standard deviations of groundwater stable isotope data with n representing the number of collected water samples. a) Growing season. b) Non-growing season.

a. Growing Season

| Groundwater Subdivision | Minimum ‰ (VSMOW) | | Maximum ‰ (VSMOW) | | Average ‰ (VSMOW) | | Standard Deviation ‰ (VSMOW) | |
|---|---|---|---|---|---|---|---|---|
| | $\delta^2H$ | $\delta^{18}O$ | $\delta^2H$ | $\delta^{18}O$ | $\delta^2H$ | $\delta^{18}O$ | $\delta^2H$ | $\delta^{18}O$ |
| Stream (n=6) | -28 | -4.8 | -27 | -4.3 | -28 | -4.6 | 0 | 0.2 |
| Water Table (n=9) | -38 | -6.5 | -22 | -3.9 | -31 | -5.4 | 6 | 1.0 |
| Alluvium Base (n=12) | -40 | -6.9 | -37 | -6.3 | -38 | -6.6 | 1 | 0.2 |
| Bedrock (n=2) | -38 | -6.4 | -37 | -6.2 | -38 | -6.3 | 1 | 0.1 |

b. Non-Growing Season

| Groundwater Subdivision | Minimum ‰ (VSMOW) | | Maximum ‰ (VSMOW) | | Average ‰ (VSMOW) | | Standard Deviation ‰ (VSMOW) | |
|---|---|---|---|---|---|---|---|---|
| | $\delta^2H$ | $\delta^{18}O$ | $\delta^2H$ | $\delta^{18}O$ | $\delta^2H$ | $\delta^{18}O$ | $\delta^2H$ | $\delta^{18}O$ |
| Stream (n=3) | -30 | -4.5 | -29 | -4.4 | -30 | -4.5 | 0 | 0.0 |
| Water Table (n=7) | -37 | -6.4 | -25 | -4.4 | -31 | -5.3 | 5 | 0.8 |
| Alluvium Base (n=11) | -40 | -6.7 | -37 | -6.3 | -38 | -6.5 | 1 | 0.1 |
| Bedrock (n=1) | -38 | -6.4 | -38 | -6.4 | -38 | -6.4 | - | - |

## LRS vs. RCS Isotopes

During the growing season, all the LRS samples were isotopically lighter compared to the RCS samples (Figure 19). The average deuterium and oxygen-18 compositions of the LRS samples were -45‰ and -6.9‰, respectively, with a *d*-excess of 10.6‰ (Appendix II). The RCS water samples were split into two groups based on differences in isotopic compositions. One RCS data group, Group A, includes the bedrock, alluvium base, and water-table D, E, and F wells (Figure 19). The average isotopic values, 38‰ for deuterium, -6.5‰ for oxygen-18, and

13.9‰ for *d*-excess, were slightly heavier compared to the LRS samples. The other RCS data group, Group B, includes water-table wells B and C and the stream samples (Figure 19). These samples exhibited the heaviest isotopic composition and were closest in value to the precipitation samples collected by Machavaram et al. (2006). The average deuterium and oxygen-18 compositions of the Group B samples were -27‰ and -4.6‰, respectively, with a *d*-excess of 9.5‰.

More variation in isotopic compositions was present during the non-growing season compared to the growing season (Figure 20). Some of the LRS samples were not isotopically lighter compared to the RCS samples; LRS shallow aquifer wells LWPH2 and LWPH4A were heavier compared to Group A (Figure 20). The LRS aquitard well samples exhibited the lightest isotopic samples (averages include $\delta^2$H: -67‰, $\delta^{18}$O: -9.0‰). The HPA samples had the next lightest average isotopes values ($\delta^2$H: -49‰, $\delta^{18}$O: -7.3‰). Group A had significantly heavier averages ($\delta^2$H: -38‰, $\delta^{18}$O: -6.5‰).

The predicted precipitation isotope compositions (calculated values) exhibit seasonal differences and are lighter at the LRS compared to the RCS (Figure 21, Appendix II). The winter and fall months (September through February) are isotopically lighter compared to the spring and summer months (March through August). Additionally, the winter and fall months plot above the GMWL, while most spring and summer months plot near or below the GMWL. The LRS precipitation values were lighter year round compared to the RCS. For example, the annual average isotope values at the LRS ($\delta^2$H: -61‰, $\delta^{18}$O: -8.5‰) compared to the RCS values ($\delta^2$H: -50‰, $\delta^{18}$O: -7.1‰).

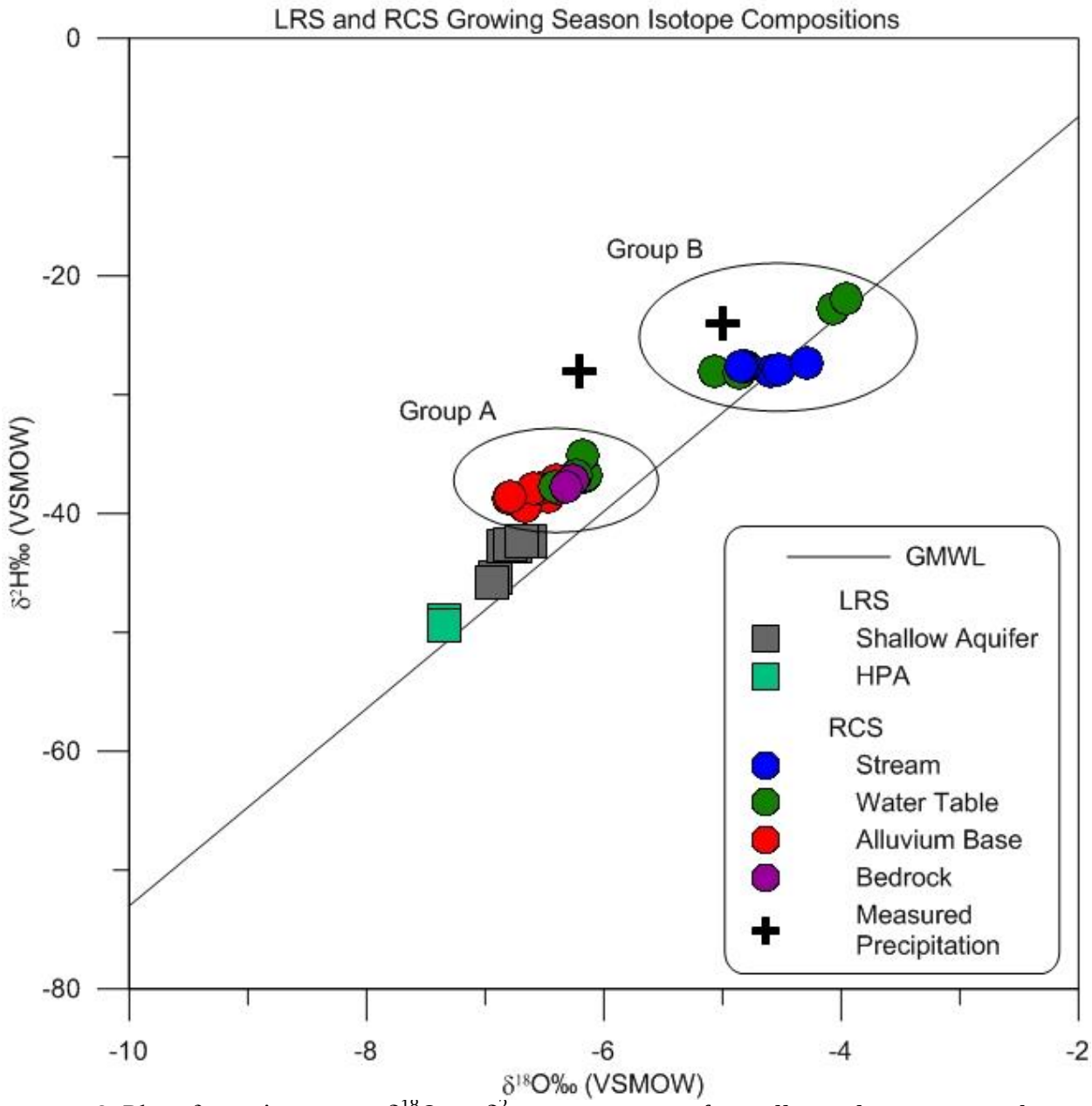


Figure 19. Plot of growing season $\delta^{18}O$ vs. $\delta^{2}H$ measurements from all sampling events at the LRS and the RCS. The measured precipitation isotope composition data were collected in May 2002 by Machavaram et al. (2006). Group A includes RCS bedrock, alluvium base, and water-table D, E, and F wells. Group B includes RCS water-table wells B and C and the stream samples.

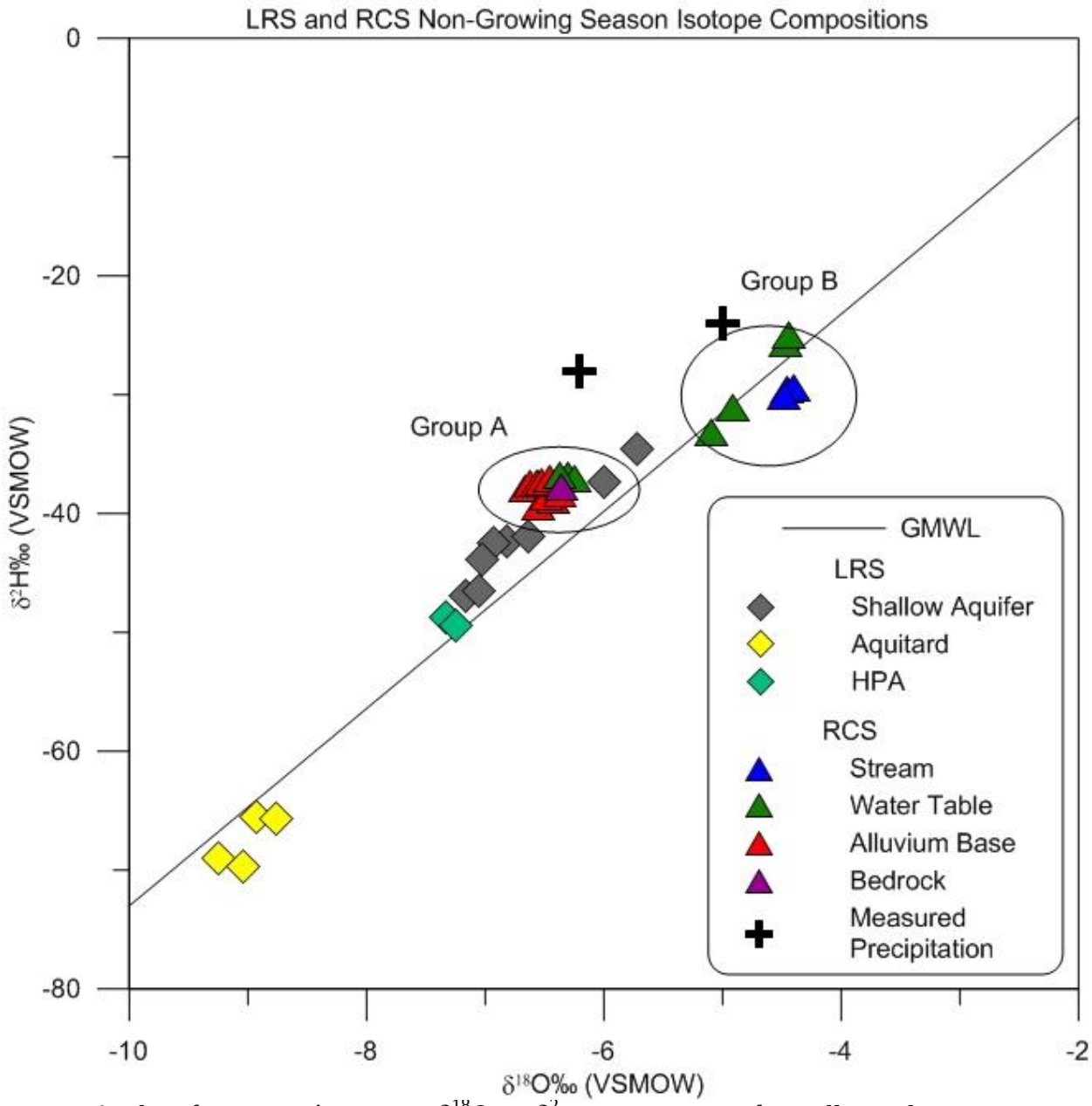


Figure 20. Plot of non-growing season $\delta^{18}O$ vs. $\delta^{2}H$ measurements from all sampling events at the LRS and the RCS. The measured precipitation isotope composition data were collected in May 2002 by Machavaram et al. (2006). Group A includes RCS bedrock, alluvium base, and water-table D, E, and F wells. Group B includes RCS water-table wells B and C and the stream samples.

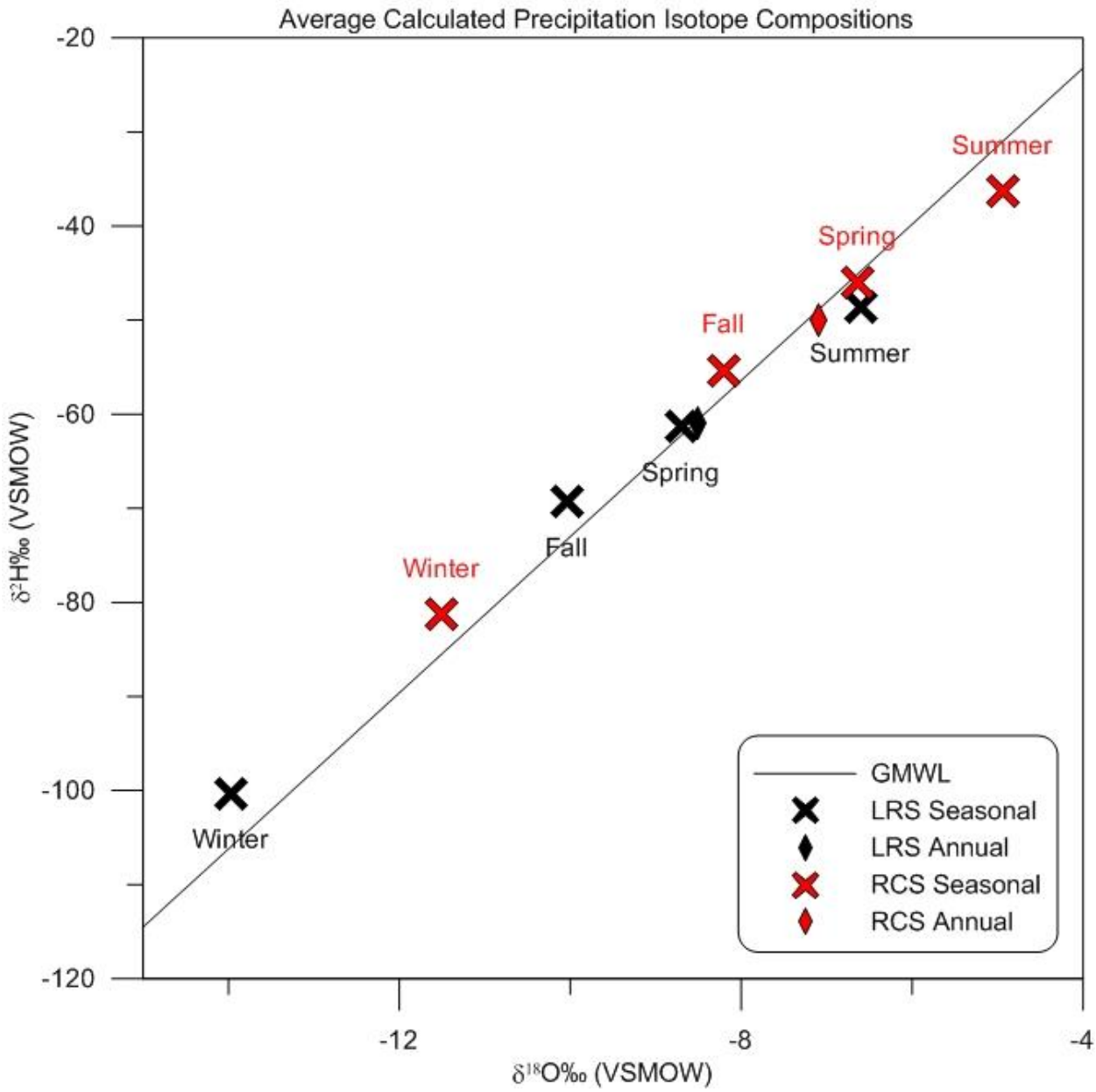


Figure 21. Plot of relative annual and seasonal average calculated precipitation isotope compositions at the LRS and RCS. Relative annual and seasonal average calculated precipitation isotope compositions were determined by the Online Isotopes Precipitation Calculator (Bowen and Revenaugh, 2003; Bowen et al., 2005; OIPC, 2014). The summer months included June, July, and August; the spring months included March, April, and May; the fall months included September, October, and November; and the winter months included December, January, and February.

# Chapter 4: Discussion

## LRS

The magnitude, duration, and intensity of precipitation events affected the subsequent amount of recharge within the subsurface of the LRS system. The largest multiday precipitation event, ending August 9, caused the shallow aquifer water level to significantly rise on August 17, with a slight rise in the water level in the aquitard well (Figure 7). The time delay between the rain event and the rise in the shallow aquifer well water level sheds light into the rate of groundwater flow through the aquifer system. In contrast, a smaller, single day precipitation event that occurred on May 30 did not result in such a large response in the shallow aquifer well water levels (0.03 to 0.05 m rise). The aquitard well water level did not exhibit any increased recovery rate after the May precipitation event. The water levels in the HPA well generally decreased after both precipitation events; the water level decreases in the HPA well are most likely a result of nearby irrigation pumping throughout the research period. Water levels in both the phreatic alluvial aquifer and the aquitard wells were not affected by the local groundwater withdrawals in the HPA.

The increased recovery rate in the aquitard well could represent the transmission of a pressure pulse from the aquifer to the aquitard (Figure 7). Aquitards are recognized for slow groundwater flow based on the sediment composition, generally clay-rich sediments (Bradbury et al., 2006; Hendry and Wassenaar, 2009; Hendry et al., 2011). However, preferential flow in aquitards can arise from layers with somewhat higher hydraulic conductivity material and the presence of vertical fractures (Cherry et al., 2006). Areas of higher hydraulic conductivity provide a groundwater flow path of lower resistance, effectively creating a preferential flow path. The LRS aquitard is considered a thin aquitard, less than 15.0 m, and thus has a higher probability of containing vertical fractures (e.g. Bradbury et al., 2006). Initial groundwater

withdrawal from an aquitard is dependent on the storage coefficient, or porewater released due to a change in head (Cherry et al., 2006). The subsequent recovery rate of the aquitard can be increased by the presence of preferential flow pathways. An additional hypothesis for the increased recovery rate of the aquitard is related to the increase in water level and pressure in the overlying shallow aquifer after the precipitation event. The higher hydraulic head and pressure from the additional groundwater storage in the shallow aquifer could result in an increase in groundwater flow to the aquitard. A combination of heterogeneous material in the aquitard, the possible presence of vertical fractures, and the large influx of groundwater into the shallow aquifer from the precipitation event are the likely causes of the increased water-level recovery rate in the aquitard well at the LRS.

Significant changes in specific conductivity measurements observed in the shallow aquifer well LWPH4A correlate to the August precipitation event and evapotranspiration (Figure 8, Appendix I). The initial decrease in specific conductance was likely a result of dilution from the influx of precipitation recharge (Figure 8, Appendix I) (e.g. Whittemore et al., 2005). As the well water level receded, the specific conductance measurements (which are corrected for temperature) could have been further affected by evapotranspiration and the vertical movement of stratified zones of different dissolved solid concentrations in the groundwater (Whittemore et al., 2005). Riparian vegetation consumes shallow groundwater via evapotranspiration; long-term groundwater specific conductance trends at the LRS exhibit a decrease between the fall and winter months and an increase in spring and summer months, indicating increased evapotranspiration activity during the growing season (Figure 8). As water is removed, salts remain behind and would cause water in the aquifer to become more saline and increase specific conductance, as observed at the LRS (Whittemore et al., 2005). The shallow aquifer LWPH4A

well screen is at a fixed depth within the aquifer (Table 1); as the groundwater level varies, stratified zones of different TDS concentrations could have fluctuated up and down, causing changes in specific conductance in the area surrounding the well screen. Other precipitation events at the LRS did not cause a significant change in specific conductance measurements. This indicates that immediate changes in specific conductance measurements at the LRS are dependent on two factors: a minimum amount of surface water recharge to dilute groundwater and fluctuations in water levels causing the vertical movement of groundwater with stratified salinity.

The spatial distance of the shallow aquifer wells LWPH4A and LWPH2 to the dry, coarse river channel could explain the effect of precipitation on the collected water-level data. These wells were located closer to the river channel than the other three shallow aquifer wells sampled (Figure 5). Precipitation in the alluvial river channel can quickly infiltrate through coarse sediment compared to the soil around the riparian zone, which would be inhibited by the interception of water by the riparian cover as well as slowed by infiltration through the root zone and thicker unsaturated zone. The coarse sediment in the river channel and its connection to coarse sediment layers in the alluvial aquifer effectively creates a preferential flow path for surface water recharge to the wells. A similar phenomenon was studied by Cook et al. (2006) at the LRS. As the groundwater level below the streambed increases, a pressure head would develop. As observed by Cook et al. (2006), shallow aquifer wells located closer to the stream, such as LWPH4A and LWPH2, would experience a greater and faster increase in water level compared to wells located further away from the stream channel due to the pressure head.

The lower geochemical concentrations and heavier isotopic measurements in the shallow aquifer wells LWPH4A and LWPH2 during the October sampling event support this hypothesis

of spatial location and infiltration effects (Figures 7 and 9-12). A precipitation event (27.69 mm) occurred two days before the sampling event (Figure 7). The geochemical concentrations from the well samples were diluted from the influx of precipitation, and the isotope compositions were lighter, possibly from intermixing with the precipitation (e.g. Coplen et al., 1999; Rein et al., 2004). The geochemical and isotope data from the November sampling event did not exhibit any effects from a precipitation event that was nine days prior (accumulation of 27.94 mm); the specific conductivity measurements were not significantly affected by the precipitation event and the geochemical and isotope values could have already recovered from the effects of precipitation infiltration through the Arkansas River channel and surrounding floodplain.

The geochemical and isotopic data for the three different units at the LRS (shallow and deep aquifers and aquitard) are dependent on the geological heterogeneities present in the subsurface. The consistency of the observed geochemical and isotopic trends indicates mixing between the shallow aquifer and HPA through a leaky aquitard system able to transfer water over a large cross-sectional area or by leakage through the gravel packs of irrigation wells that connect the alluvial aquifer and underlying HPA (Figures 9-11) (e.g. Butler et al., 2004, Fetter, 2001). The alluvial aquifer had higher dissolved ion concentrations compared to the HPA. However, well LWPH4B, which is in the lower part of the alluvial aquifer and the closest in vertical depth of the alluvial aquifer wells to the HPA well, consistently had lower constituent concentrations and lighter isotopic compositions compared to the shallower aquifer wells. Although the dissolved constituent concentrations at this well were consistently lower, the magnitude of difference for each dissolved constituent varied between sampling events.

The isotopic compositions of the well samples became lighter with depth, excluding the aquitard well samples (Figure 12). This resembles the critical zone theory defined by Clark and

Fritz (1997). The isotopic signature of surface water recharge to groundwater is dependent on the isotopic composition of precipitation, with variations based on groundwater mixing of additional water sources and seasonal recharge (e.g. Gibson et al., 2005; O'Driscoll et al., 2005). Thus, shallow groundwater isotope compositions generally fluctuate around the mean annual precipitation compositions with fewer seasonal variations at depth (Clark and Fritz, 1997; O'Driscoll et al., 2005). Well LWPH4B exhibited the lightest isotope compositions in the alluvial aquifer (Figure 12); specifically, the isotope compositions of this well were close to the composition of the HPA samples. The similarity between the dissolved constituent concentrations and isotopic compositions of the HPA well and the LWPH4B well, regardless of the sampling season or recent precipitation events, suggests groundwater intermixing between the two aquifers zones through aquitard heterogeneities or water movement through the gravel packs of irrigation wells.

The isotopic data suggests the longest water storage occurred in the aquitard at the LRS. Aquitards can contain water with an isotopic signature representative of the climatic conditions from when the aquitard was formed (Bradbury et al., 2006). The isotopic signature of the older porewater would be different compared to the present day precipitation isotopic signature; the isotopic signature of the porewater contained within the LRS aquitard is different compared to the phreatic alluvial aquifer and HPA isotopic signatures (which have been affected in the recent by surface water recharge), indicating the water in the aquitard originated from a different time period. The consistency of the isotope values in all samples from the aquitard indicated no mixing or influence from the waters in the overlying and underlying aquifers. This suggests older water is held within the aquitard compared to the two aquifers.

Surface water recharge to groundwater at the LRS was indicated by seasonal changes in isotopic compositions. Precipitation isotopic compositions are a function of the changing seasonal climate relative to several environmental factors including temperature, humidity, and altitude (Blasch and Bryson, 2007; Coplen et al., 1999). The calculated isotopic composition of winter precipitation at both sites was lighter compared to summer precipitation (Figure 21); this trend is typical in the North American Interior (e.g. Reddy et al., 2006). A comparison of the annual and seasonal calculated precipitation isotope compositions to the groundwater samples at the LRS indicate that the time of the recharge likely occurred during the summer and spring months (Figure 12). The winter and fall isotopic compositions were lighter compared to the alluvial aquifer and HPA samples, indicating recharge did not occur in the winter and fall. The year round shallow aquifer isotope compositions are similar in composition to the summer calculated precipitation, which further suggests the seasonal timing of groundwater recharge likely occurred during the summer months. However, the isotope compositions of the aquitard well samples were located between the spring and fall isotopic compositions, suggesting that the aquitard is not affected by the groundwater recharge or contains older water indicative of previous stream stage, recharge, and climatic conditions.

**RCS**

Water levels in all of the water-table wells exhibited an immediate rise due to precipitation events with water-table well F being most affected (Figure 14). During two precipitation events, in May and August, the water level in water-table well F rose above and then fell below the level of the pressure transducer in the well. Only a single sample could be collected during visits to the site for this study, which was in September shortly after the August

precipitation event. While collecting the water sample, the water level immediately decreased during pumping and proceeded to recover in a short time period.

The source of water-level fluctuations in water-table well F could result from precipitation infiltration, lateral groundwater movement of stream-bank recharge through the more permeable layers to the well location, or vertical flow from deeper in the alluvium. Vertical flow from deeper in the alluvium could be from the water pressure from bank storage that did not reach the well, the pressure in the underlying bedrock aquifer after an increase in water level from precipitation recharge in the upland area, or both of these mechanisms. The main source of the water for the water-table well F sample was from vertical flow from deeper in the alluvium as evident from the closer similarity of the isotope data for the water-table well F sample to that of the alluvium base well samples than to that of the stream water and water-table wells B and C (Figure 18). The TDS and chloride concentrations in the water-table well F sample were the highest of any samples collected from the RCS, and the sulfate concentration was also relatively high (Figures 15 and 17, Appendix I). The water rising from lower in the alluvium could have dissolved precipitated salts in the unsaturated zone of the soil around water-table well F that had accumulated from evapotranspiration consumption of groundwater and soil moisture. Similar increases in TDS concentrations have been observed in previous studies at the RCS (Whittemore et al., 2005).

The spatial locations of the water-table wells could have affected the nitrate concentrations observed in each water-table well. The nitrate concentrations were too low to show any effects of dilution from precipitation, except for concentrations in water-table well D (Figure 16). Water quality is dependent on varying factors at different spatial scales (Allan 2004; Dent et al. 2001; Johnson et al. 1997). Water-table well D is located furthest from the stream and

closest in proximity to the hay and agricultural fields (Figure 6). Higher nitrate concentrations in this well could have been caused by the application of fertilizer on the agricultural fields, nitrification and denitrification processes in the riparian zone, or the recycling of detritus material left on the edge of the field after cutting the hay (e.g. Canfield et al., 2010; Delgado and Follet, 2002). Denitrification and nitrification processes were not studied further since dissolved oxygen measurements were not collected. Another hypothesis is that nitrate dilution occurred in all water-table wells, except water-table well D, from the infiltration of cleaner stream water. In comparison, the chloride concentrations, which are considered a conservative tracer, did not exhibit the same trends as the nitrate concentrations at the RCS water-table wells (Appendix I). This indicates that the water-table well F nitrate concentrations were affected by an unidentified source.

The alluvium base and bedrock well samples generally exhibited the same geochemical and isotopic values due to similar well screen depths and the upwelling of groundwater from the bedrock (Figure 15-18, Table 2). The base of the alluvium and the top of the bedrock are roughly 6.0 m below the land surface. The alluvium base wells were screened into the top centimeters of the weathered bedrock for increased water availability during sample collection (Table 2). The limestone bedrock includes thin beds and filled fractures of gypsum that could have dissolved with groundwater contact, creating small cavities and increased porosity. The cavities would then allow for preferential limestone dissolution along these more permeable paths of groundwater flow; this was indicated during drilling of the bedrock well when the drill bit suddenly dropped in a couple zones, indicating voids or cavities within the bedrock (Donald Whittemore, Kansas Geological Survey, personal communication). Similar water would be observed in the interconnected voids and in solution-widened fractures throughout the bedrock, and thus similar

geochemical and isotopic data for the alluvium base and bedrock wells would also be observed. Generally, deep groundwater isotopic compositions are affected by dilution or mixing with other waters (Huddart et al., 1999). The similar isotopic compositions of the alluvium base and bedrock samples indicate mixing between the two reservoirs of water. Additionally, these samples were located slightly above the GMWL, possibly due to groundwater-mineral interactions (IAEA, 1983).

Seasonal effects were observed in stream and water-table well samples, which offer insight into the residence time of groundwater at the RCS. Stream samples were heavier in isotopic composition than all groundwater samples (excluding water-table wells B and C), close in proximity to the measured precipitation isotope compositions, and generally below the GMWL (Figure 18). The surface water isotopic signature is reliant on precipitation, evaporation, and groundwater discharge (e.g. Darling et al., 2003; Gibson et al., 2005). Specifically, during the evaporation process, lighter isotopes evaporate before heavy isotopes, causing the residual water to become enriched in heavy isotopic species (e.g. Gibson et al., 2005; Krabbenhoft et al., 1990). Water-table wells B and C were closest in isotopic composition to the stream compared to all other sampling locations. Additionally, the samples varied in composition based on seasonal changes, which are generally seen in isotopes above the water table and shallow groundwater (Clark and Fritz, 1997). The variations in isotopic composition could result from a slight evaporation effect or variability in the environmental factors governing the precipitation isotope concentrations. Regardless, the isotope measurements reveal the connectivity between the surface water and shallow groundwater in some portions of the alluvium. The stream and water-table wells B and C represent short-term water storage; the isotopic compositions varied with each sampling event based on changing seasonal changes, source of water (precipitation or

stream base flow), and spatial location. In contrast, the deeper alluvium base, bedrock, and water-table D, E, and F well samples did not exhibit any changes in isotopic composition due to precipitation events, and represent longer-term water storage (Figure 18).

Surface water recharge to groundwater can be monitored by seasonal changes in precipitation, surface water, and groundwater isotopic compositions. A comparison of the annual and seasonal calculated precipitation isotope compositions to the groundwater samples at the RCS indicated that the time of the recharge likely occurred during the summer and spring months (Figure 18). The winter and fall calculated precipitation isotope compositions were lighter compared to the groundwater samples, likely indicating a lack of influence of winter and fall recharge on the groundwater. The stream and water-table well B and C isotope compositions were similar to those for the summer calculated precipitation, which suggests the likely influence of summertime groundwater recharge. The bedrock, alluvium base, and water-table wells D, E, and F exhibited more constant isotopic compositions among seasons and were closer to the spring calculated precipitation. The lack of seasonal variation further supports longer-term water storage in the alluvial base, bedrock, and water-table D, E, and F wells compared to the stream and water-table wells B and C.

## LRS vs. RCS Groundwater-Surface Water Interactions

Interactions between surface water and shallow groundwater were present at both the LRS and RCS. The effect of surface water on groundwater varied based on stream stage, subsurface geology, and seasonality at each site. The presence of groundwater-surface water connections will help show possible recharge and contamination pathways.

The large May and August precipitation events affected the LRS and RCS with roughly the same magnitude, duration, and intensity. The Arkansas River bed at the LRS acted as a preferential pathway for surface water recharge to shallow groundwater. Infiltrated surface water increased shallow aquifer well water levels with little effect on the deeper wells in the aquitard and HPA (Figure 7); the aquitard acted as a geologic barrier inhibiting rapid surface water infiltration and groundwater to the HPA. In contrast, precipitation runoff accumulated in the Rock Creek river channel, increased stage height, infiltrated the stream banks, and caused groundwater to laterally flow to and from the observation wells. All observation wells at the RCS were affected, to a varying degree, by large precipitation events; smaller well water-level variations in response to the precipitation events were observed in the bedrock and alluvium wells compared to the water-table wells (Figure 14).

The shallow groundwater wells at the LRS and RCS did exhibit seasonal variations in geochemical and isotopic values compared to the deeper groundwater wells (Figures 9-12 and 15-18). These factors further indicate that surface and groundwater interactions are present at both sites. Although the aquitard is considered a leaky aquitard, the connection between surface water and deep HPA groundwater was not as prominent compared to the interactions of surface water and shallow alluvial aquifer groundwater (based on the seasonal geochemical and isotopic variations) (Figures 9-12). The lighter isotopic composition of the aquitard well samples indicates older water stored within the aquitard. In contrast, the RCS bedrock and alluvium base wells exhibited little to no seasonal variations compared to the surface and water-table well (Figures 15-18). The sediment-groundwater interface and spatial location of each water-table well to the stream channel affected the effect of stream water on shallow groundwater. The

seasonal variations in the individual water-table well samples provide insight to differing subsurface heterogeneities and subsequent effects of surface water on the shallow groundwater.

Increased concentrations of dissolved solids were observed at both sites, most likely a result of transpiration. A dry period affected the LRS and RCS prior to the sample collections in this research. As the groundwater table dropped, stratified zones of concentrated salts formed (e.g. Whittemore et al., 2005). Consumption of the groundwater from plant root uptake caused the stratified zones to become more concentrated in salts. Isotopic compositions of the groundwater samples at the LRS and RCS did not exhibit a significant deviation below the GMWL, indicating that evaporation did not appear to be a major factor in increasing the concentration of dissolved constituents from season to season. Transpiration does not significantly change the isotopic composition of water and could have potentially been a major factor in the stratified zones of concentrated salts (Clark and Fritz, 1997). As the groundwater table rose, due to a large precipitation event, the water table reached the stratified zones of concentrated salts and resulted in increased concentrations of dissolved solids at both research sites.

Isotopic signatures of surface and groundwater samples indicate relative groundwater storage durations at the LRS and RCS. Several factors can affect precipitation isotope compositions, including latitude, altitude, temperature, precipitation, relative humidity, and evaporation (Clark and Fritz, 1997; Coplen et al., 1999). These factors could explain the differences in the isotope compositions between the short-term water storage of the RCS water-table B and C wells (Group B) versus the longer-term water storage at the LRS and remaining RCS locations (Group A) (Figures 19-20). The RCS calculated precipitation isotope compositions were on average 15‰ enriched in deuterium and 2‰ enriched in oxygen-18

compared to the LRS calculated precipitation isotope values (Figure 21). This trend was consistent with the surface and groundwater isotope compositions determined at both sites; the RCS Group B samples, representing short-term water storage, were roughly 10‰ enriched in deuterium and 2‰ enriched in oxygen-18 compared to the remaining RCS (Group A) and LRS groundwater samples, which represented longer-term water storage (Figures 19-20). The RCS alluvium base and bedrock samples fall within the isotopic range of the LRS shallow aquifer samples. The LRS aquitard samples are much lighter in comparison, indicating a different source of water. The LRS aquitard and HPA samples did not exhibit as much variability compared to the shallow groundwater at both site, which indicates no effects from seasonal variations.

## Chapter 5: Conclusion

This research compared two locations with differing subsurface geologic environments and somewhat different climates to assess changes in groundwater-surface water interactions. The influence of surface water on groundwater varied at each site relative to stream stage, subsurface heterogeneity, and seasonal changes. The different surface water connections with groundwater indicate that specific site conditions are important considerations for safeguarding the future quantity and quality of water in the aquifers. The knowledge obtained from this research could help determine possible recharge and contaminant flow paths of other aquifers located in similar alluvial environments.

The geochemical variation between the shallow and deep aquifers and aquitard at the LRS implied a leaky aquitard system with longer-term water storage in the aquitard. Similar dissolved solids and isotope values provide evidence for a connection between the shallow and deep aquifers through the heterogeneities present in the aquitard and flow through the gravel packs of nearby irrigation wells. The deepest well in the shallow alluvial aquifer had similar

isotopic composition to the deep HPA well, further supporting possible mixing between the deep aquifer water and shallow aquifer water. However, the hydraulic and chemical response to precipitation and pumping indicates that the aquitard acts as a geologic barrier between the shallow alluvial aquifer and deeper HPA by inhibiting rapid water level changes in one aquifer from affecting the other. The lower dissolved solid concentrations in the LRS aquitard could have resulted from the retention of fresher water by the low hydraulic conductivity of the aquitard. The isotopic signatures in the aquitard were significantly lighter compared to both aquifers. Combined with the geochemical data, this indicates older, fresher water contained within the aquitard compared to the shallow and deep aquifers. The hydrologic connection between the two aquifers signifies recharge pathways and the potential for contamination pathways between the two aquifers.

Spatial location, subsurface heterogeneity, and surface water infiltration are the primary causes of variations, indicative of the distinction between short-term and long-term water storage, in the observed well data at different locations at the RCS. The varying values indicate surface water and shallow groundwater interactions through the lateral groundwater movement of surface water recharge through the more permeable layers at selected locations. Dissolved constituent concentrations and stable isotope compositions exhibited the highest variation in the stream and water-table samples between the growing and non-growing season, indicating short-term water storage. In contrast, the consistency of the deeper groundwater, despite precipitation and seasonal changes, implied longer-term storage. The varying subsurface geology allows for vulnerability of groundwater to contamination pathways when the groundwater was directly influenced by surface water recharge in parts of the alluvium. The low permeability of the alluvium and the higher piezometric level of groundwater in the shallow bedrock aquifer than at

the water table protect the bedrock aquifer from potential contamination by stream water.

Stratified zones of concentrated salts at both the LRS and RCS sites were primarily a result of transpiration. Increasing concentrations of dissolved solids were observed at both sites. The isotopic composition of the groundwater samples did not exhibited significant deviations below the GMWL, indicating that evaporation was not a major factor in the increased concentrations of dissolved constituents. This suggests that increases in dissolved constituent concentrations observed during dry periods at the LRS and RCS are primarily controlled by the process of transpiration; as the groundwater is withdrawn from the water table, stratified zones of concentrated salts remain in a smaller volume of soil moisture and groundwater.

## Chapter 6: Future Work

Additional groundwater sampling during growing and non-growing seasons would improve the determination of regional long-term trends. Long-term changes in climate would affect stream stage and alter the isotopic composition of precipitation. Understanding the effect of varying environmental factors, such as long-term drought conditions and temperature, would further the breadth of knowledge of surface and groundwater connections. Additionally, the long-term collection of stream water isotope data could provide a local meteoric water line for the study regions.

Additional data for seasonal oxygen-18 compositions would provide a means to determine the mean residence time (MRT) of groundwater at both field sites. Relative groundwater residence times were determined at the LRS and RCS sites. McGuire et al. (2002) and Reddy et al. (2006) combined precipitation oxygen-18 values and sine function models that characterized groundwater flow to determine the MRT of groundwater. The sine function

utilized in these studies would be applied to the measured oxygen-18 compositions at the LRS and RCS to strengthen the understanding surface-groundwater interactions. Analysis of MRT estimations from both equations would provide comparative values. Additionally, understanding the mean residence time of groundwater enhances the predictions of aquifer vulnerability to groundwater contamination (McGuire et al., 2002). The establishment of long-term surface and groundwater sampling would need to be established for the application of MRT estimations.

## References


Aji, K., Tang, C., Song, X., Kondoh, A., Sakura, Y., Yu, J., Kaneko, S. (2008) Characteristics of chemistry and stable isotopes in groundwater of Chaobai and Yongding River basin, North China Plain. Hydrological Processes 22:63-72. doi: 10.1002/hyp.6640

Allan, J. D. (2004) Landscapes and riverscapes: the influence of land use on stream ecosystems. Annual review of ecology, evolution, and systematics 34:257-284.

Alley, W. M., Healy, R. W., LaBaugh, J.W., Reilly, T.E. (2002) Flow and storage in groundwater systems. Science 296(5575):1985-1990. doi: 10.1126/science.1067123

Alley, W.M., Reilly, T.E., Franke, O.L. (1999) Sustainability of ground-water resources. U.S. Geological Survey Circular 1186.

Blasch, K.W., Bryson, J.R. (2007) Distinguishing sources of ground water recharge by using $\delta^2H$ and $\delta^{18}O$. Ground Water 45(3):294-308.

Bowen G. J. and Revenaugh J. (2003) Interpolating the isotopic composition of modern meteoric precipitation. Water Resources Research 39(10), 1299, doi:10.129/2003WR002086.

Bowen G. J., Wassenaar L. I. and Hobson K. A. (2005) Global application of stable hydrogen and oxygen isotopes to wildlife forensics. Oecologia 143, 337-348, doi:10.1007/s00442-004-1813-y.

Bradbury, K.R., Gotkowitz, M.G., Hart, D.J., Eaton, T.T., Cherry, J.A., Parker, B.L., Borchardt, M.A. (2006) Contaminant Transport Through Aquitards: Technical Guidance for Aquitard Assessment, 144p.

Butler, J.J., Jin, W., Mohammed, G.A., Reboulet, E.C. (2011) New insights from well responses to fluctuations in barometric pressure. Groundwater 49(4):525-533.

Butler, J.J., Kluitenberg, G.J., Whittemore, D.O., Loheide, II, S.P., Jin, W., Billinger, M.A., Zhan, X. (2007) A field investigation of phreatophyte-induced fluctuations in the water table. Water Resources Research 43:W02404. doi:10.1029/2005WR004627.

Butler, J.J., Whittemore, D.O., Zhan, X., Healey, J.M. (2004) Analysis of two pumping tests at the O'Rourke Bridge site on the Arkansas River in Pawnee County, Kansas, Kansas Geological Survey Open File Report, 2004– 32, 58 pp.

Canfield, D.E., Glazer, A.N., Falkowski, P.G. (2010) The evolution and future of Earth's nitrogen cycle. Science 330:192-196.

Cherry, J.A., Parker, B.L, Bradbury, K.R., Eaton, T.T., Gotkowitz, M.G., Hart, D.J., Borchardt, M.A. (2006) Contaminant Transport Through Aquitards: A State-of-the-Science Review, 126p.

Choi, B., Yun, S., Mayer, B., Chae, G., Kim, K., Kim, K., Koh, Y. (2010) Identification of groundwater recharge sources and processes in a heterogeneous alluvial aquifer: results from multi-level monitoring of hydrochemistry and environmental isotopes in a riverside agricultural area in Korea. Hydrological Processes 24:317-330. doi: 10.1002/hyp.7488

Clark, I. D., Fritz, P.L. (1997) Environmental Isotopes in Hydrogeology. Lewis, Boca Raton, 328 p.

Cook, A., Geyer, T., Shook, G., Butler, Jr., J.J., Whittemore, D.O., Kluitenberg, G.J. (2006) Focused recharge in a semi-arid riparian zone. Eos, 87 (52), Fall Meet. Suppl., Abstract H11A-1222.

Coplen, T.B., Herczeg, A.L., Barnes, C. (1999) Isotope engineering – using stable isotopes of the water molecule to solve practical problems *in* Cook, P.G., Herczeg, A.L. eds., Environmental Tracers in Subsurface Hydrology. Kluwer Academic: Boston, 80-110.

Darling, W.G., Bath, A.H., Talbot, J.C. (2003) The O & H stable isotopic composition of freshwaters in the British Isles. 2. Surface waters and groundwater. Hydrology and Earth System Sciences 7(2):183-195.

Delgado, J.A., Follett, R. F. (2002) Nitrogen fate and transport in agricultural systems. Journal of Soil and Water Conservation 57(6):402-414.

Dent, C. L., Grimm, N. B. (1999) Spatial heterogeneity of stream water nutrient concentrations over successional time. Ecology 80(7):2283-2298.

Fetter, C.W. (2001) Applied Hydrogeology 4$^{th}$ edition: New Jersey, Prentice Hall, 95-98 p.

Gibson, J.J., Edwards, T.W.D., Birks, S.J., St Amour, N.A, Buhay, W.M., McEarchern, P., Wolfe, B.B., Peters, D.L. (2005) Progress in isotope tracer hydrology in Canada. Hydrological Processes 19:303-327. doi: 10.1002/hyp.5766

Gleeson, T., Novakowski, K., Cook, P.G., Kyser, K.T. (2009) Constraining groundwater discharge in a large watershed: Integrated isotopic, hydraulic, and thermal data from the Canadian shield. Water Resources Research 45:W08402. doi:10.1029/2008WR007622

Hendry, M.J., Barbour, S.L., Zettl, J., Chostner, V., Wassenaar, L.I. (2011) Controls on the long-term downward transport of $\delta^2$H of water in a regionally extensive, two-layered aquitard system. Water Resources Research 47:W06505.

Hendry, M.J., Wassenaar, L.I. (2009) Inferring heterogeneity in aquitards using high-resolution δD and $\delta^{18}$O profiles. Groundwater 47(5):639-645.

Huddart, P.A., Longstaffe, F.J., Crowe, A.S. (1999) δD and $\delta^{18}$O evidence for inputs to groundwater at a wetland coastal boundary in the southern Great Lakes region of Canada. Journal of Hydrogeology 214:18-31.

IAEA (1983) Isotope techniques in the hydrogeological assessment of potential sites for the disposal of high-level radioactive wastes. Technical Report Series, No. 228.

Johnson, L. B., Richards, C., Host, G. E., Arthur, J. W. (1997) Landscape influences on water chemistry in Midwestern stream ecosystems. Freshwater Biology 37:193-208.

Kansas Geological Survey (1996) KGS Special Maps 2 and 3 – Geologic Map of Kansas. http://www.kgs.ku.edu/General/geolSheetMap.html (accessed September 2012).

Kansas State University (2014) Historical Weather: http://mesonet.k-state.edu/weather/historical/#! (accessed July 2014).

Krabbenhoft, D.P., Bowser, C.J., Anderson, M.P., Valley, J.W. (1990) Estimating groundwater exchange with lakes 1. The stable isotope mass balance method. Water Resources Research 26(10):2445-2453.

Kendall, C., Coplen, T.B. (2001) Distribution of oxygen-18 and deuterium in river waters across the United States. Hydrological Processes 15:1363-1393.

Ladouche, B., Probst, A., Viville, D., Idir, S., Baque, D., Loubet, M., Probst, J.L., Bariac, T. (2001) Hydrograph separation using isotopic, chemical, and hydrological approaches (Strengbach catchment, France). Journal of Hydrology 242(3-4):255-274.

"Larned." 38°12'11.52"N and 99°00'08.61"W. GOOGLE EARTH. April 10, 2014. July 3, 2014.

Machavaram, M.V., Whittemore, D.O., Conrad, M.E., Miller, N.L. (2006) Precipitation induced stream flow: an event based chemical and isotopic study of a small stream in the Great Plains region of the USA. Journal of Hydrology 330:470-480

McCarthy, K.A., McFarland, W.D., Wilkinson, J.M., White, L.D. (1992) The dynamic relationship between ground water and the Columbia River: using deuterium and oxygen-18 as tracers. Journal of Hydrology 135:1-12.

McGuire, K.J., DeWalle, D.R., Gburek, W.J. (2002) Evaluation of mean residence time in subsurface waters using oxygen-18 fluctuations during drought conditions in the mid-Appalachians. Journal of Hydrology 261:132-149.

O'Connor, D.R. (2002) Report of the Walkerton Inquiry; the events of May 2000 and related issues. Ontario Ministry of the Attorney Genery, Toronto, Ontario, Parts 1 and 2, 1280p.

O'Driscoll, M.A., DeWalle, D.R., McGuire, K.J., Gburek, W.J. (2005) Seasonal $^{18}O$ variations and groundwater recharge for three landscape types in central Pennsylvania, USA. Journal of Hydrology 303:108-124.

OIPC (2014) OIPC: The Online Isotopes in Precipitation Calculator: http://wateriso.utah.edu/waterisotopes/pages/data_access/oipc.html (accessed July 2014).

Ray, C., Soong, T.W., Lian, Y.Q., Roadcap, G.S. (2002) Effect of flood-induced chemical load on filtrate quality at bank filtration sites. Journal of Hydrology 266:235-258.

Reddy, M.M., Schuster, P., Kendall, C., Reddy, M.B. (2006) Characterization of surface and ground water $\delta^{18}O$ seasonal variation and its use for estimating groundwater residence times. Hydrological Processes 20:1753-1772.

Rein, A., Hoffmann, R., Dietrich, P. (2004) Influence of natural time-dependent variations of electrical conductivity on DC resistivity measurements. Journal of Hydrology 285:215-232.

Sheets, R.A., Darner, R.A., Whitteberry, B.L. (2002) Lag times of bank filtration at a well field, Cincinnati, Ohio, USA. Journal of Hydrology 266:162-174.

Schubert, J. (2002) Hydraulic aspects of riverbank filtration – field studies. Journal of Hydrology 266:145-161.

Teles, V., Delay, F., de Marsily, G. (2004) Comparison of genesis and geostatistical methods for characterizing the heterogeneity of alluvial media: Groundwater flow and transport simulations. Journal of Hydrology 294:103-121.

University of Colorado, Kansas Geological Survey (2013) Collaborative Research: Refinement of techniques for estimating evapotranspiration from narrow riparian zones – water balance and atmospheric measurements. Final Report, NSF Award Numbers: 0741419 (KGS), 0741397 (CU Boulder).

USEPA (1998) National Primary Drinking Water Regulations: Interim Enhanced Surface Water Treatment. Federal Register Rules and Regulations 63(241):69477-69521.

Vries, J.J., Simmers, I. (2002) Groundwater recharge: an overview of processes and challenges. Hydrogeology Journal 10:5-17.

Whittemore, D.O., Butler, J.J., Jr., Healey, J.M., McKay, S.E., Aufman, M.S., Brauchler, R. (2005) The Impact of stream-aquifer interactions on ground-water quality in the alluvial aquifer of the middle Arkansas River. Proceedings 22nd Annual Water and Future of Kansas Conf., Topeka, KS, p. 37.

Whittemore, D.O., Butler, J.J. Jr., Reboutlet, E.C, Rajaram, H., Solis, J.A., Stotler, R.L., Knobbe, S., Dealy, M.T. (2012) Contrasts in stream-aquifer interactions driven by hydrogeology and geomorphology. Presentation presented at the Geological Society of America Annual Meeting, Charlotte, NC, USA November 2012.

Winter, T.C., Harvey, J.W., Franke, O.L., Alley, W.M. (1998) Ground water and surface water a single resource. U.S. Geological Survey Circular 1139.

## Appendix I. Additional Figures

Figure 22. Groundwater collection at the LRS during November 2012. (Photo credit: Randy Stotler).

Figure 23. Arkansas River at the LRS during November 2012. (Photo credit: Molly Long).

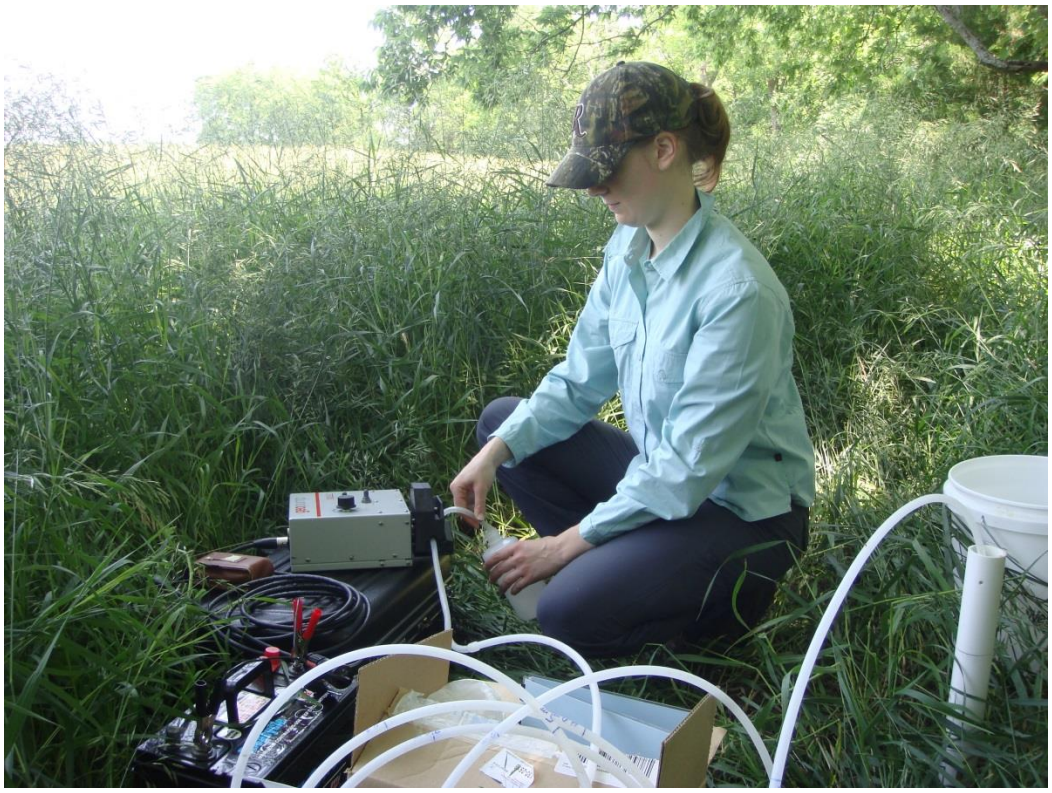

Figure 24. Groundwater collection at the RCS during June 2013. (Photo credit: Donald Whittemore).

Figure 25. Surface water collection at the RCS during July 2013 (Photo credit: Molly Long).

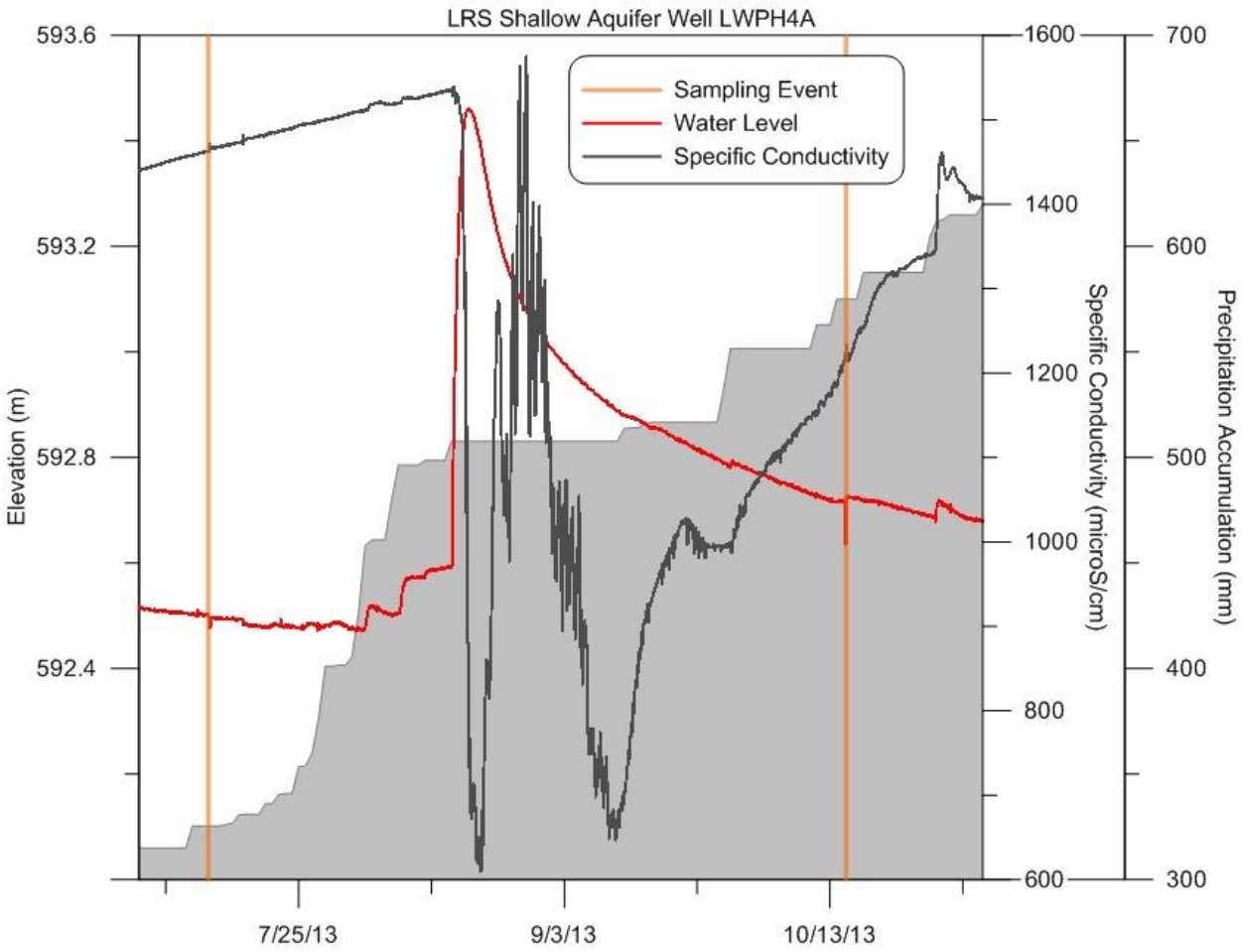


Figure 26. Groundwater elevations and corresponding specific conductivity for the LRS shallow aquifer well LWPH4A. Precipitation data, represented by the shaded gray area, is a cumulative total of daily accumulation. The water levels were recorded every fifteen minutes. Well elevations have been surveyed; the units are meters AMSL.

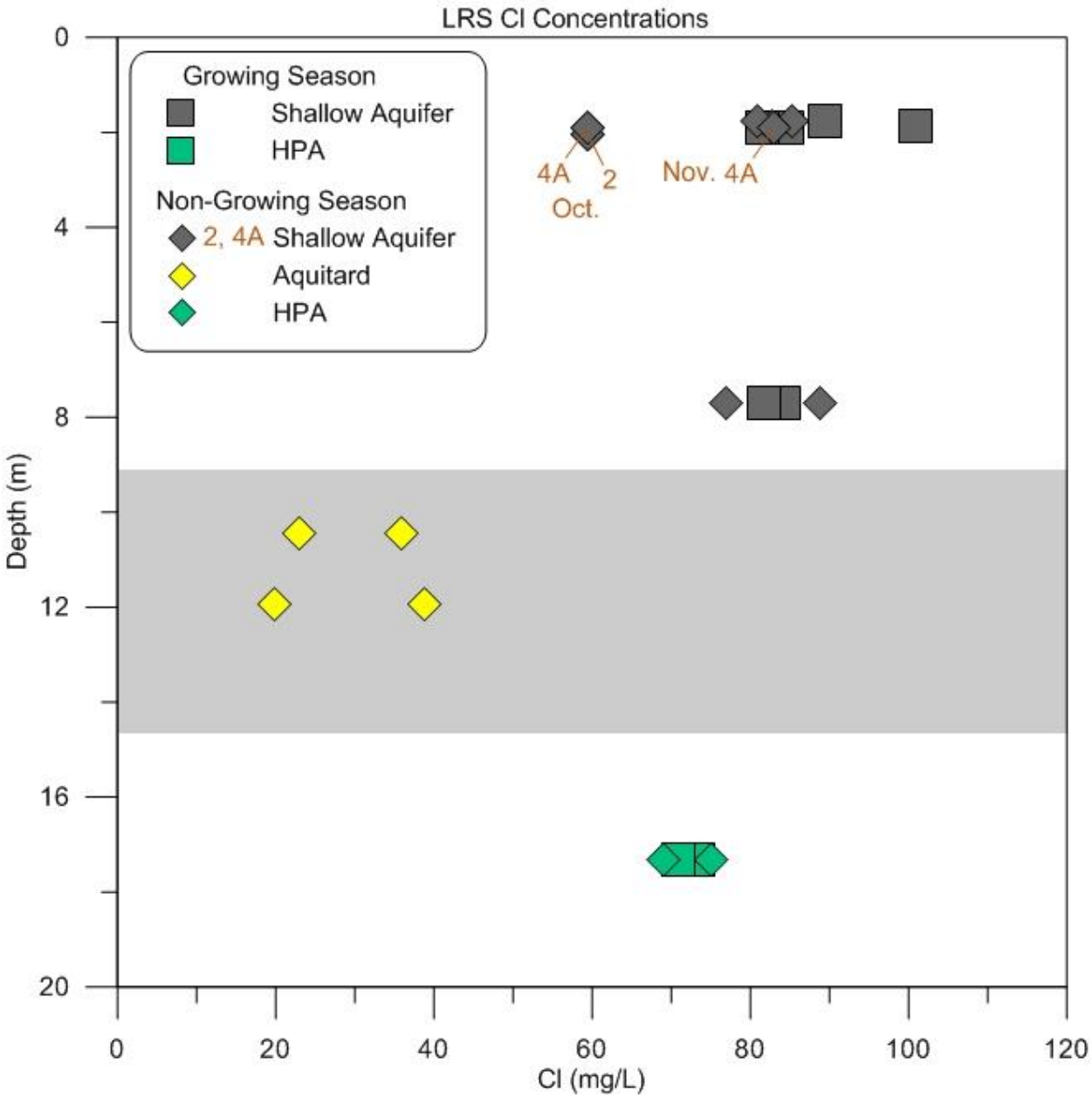


Figure 27. Chloride concentrations vs. average well screen depth at the LRS. The shaded gray area represents the approximate location of the aquitard (aquitard thickness varies from 3.1 to 6.6 m across the study area).

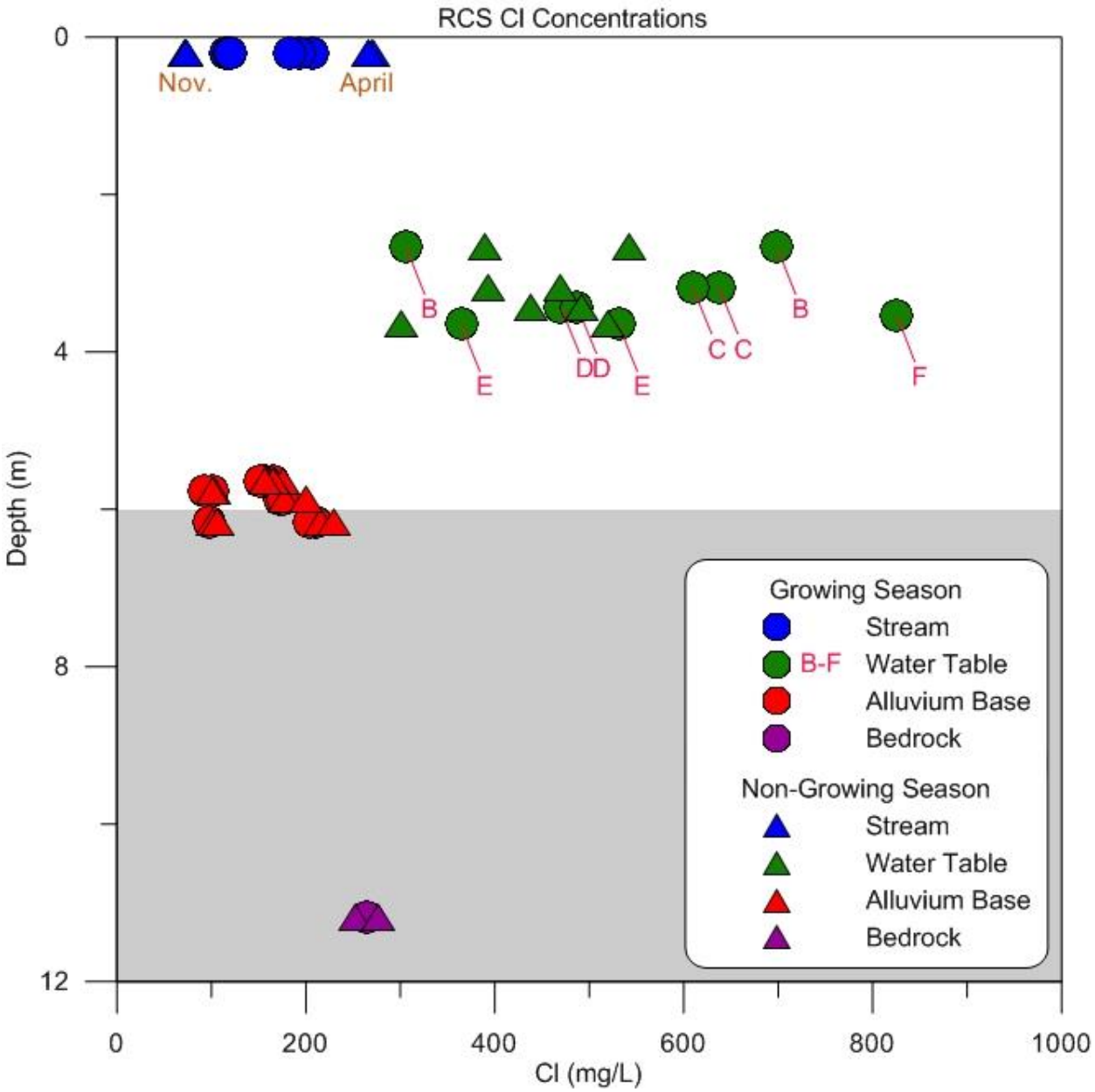


Figure 28. Chloride concentrations vs. average well screen depth at the RCS. The shaded gray area represents the approximate location of the bedrock (depth to the bedrock varies between 5.5 and 7.6 m below the land surface across the study area). Stream samples are located at a depth of 0.2 m for clarity.

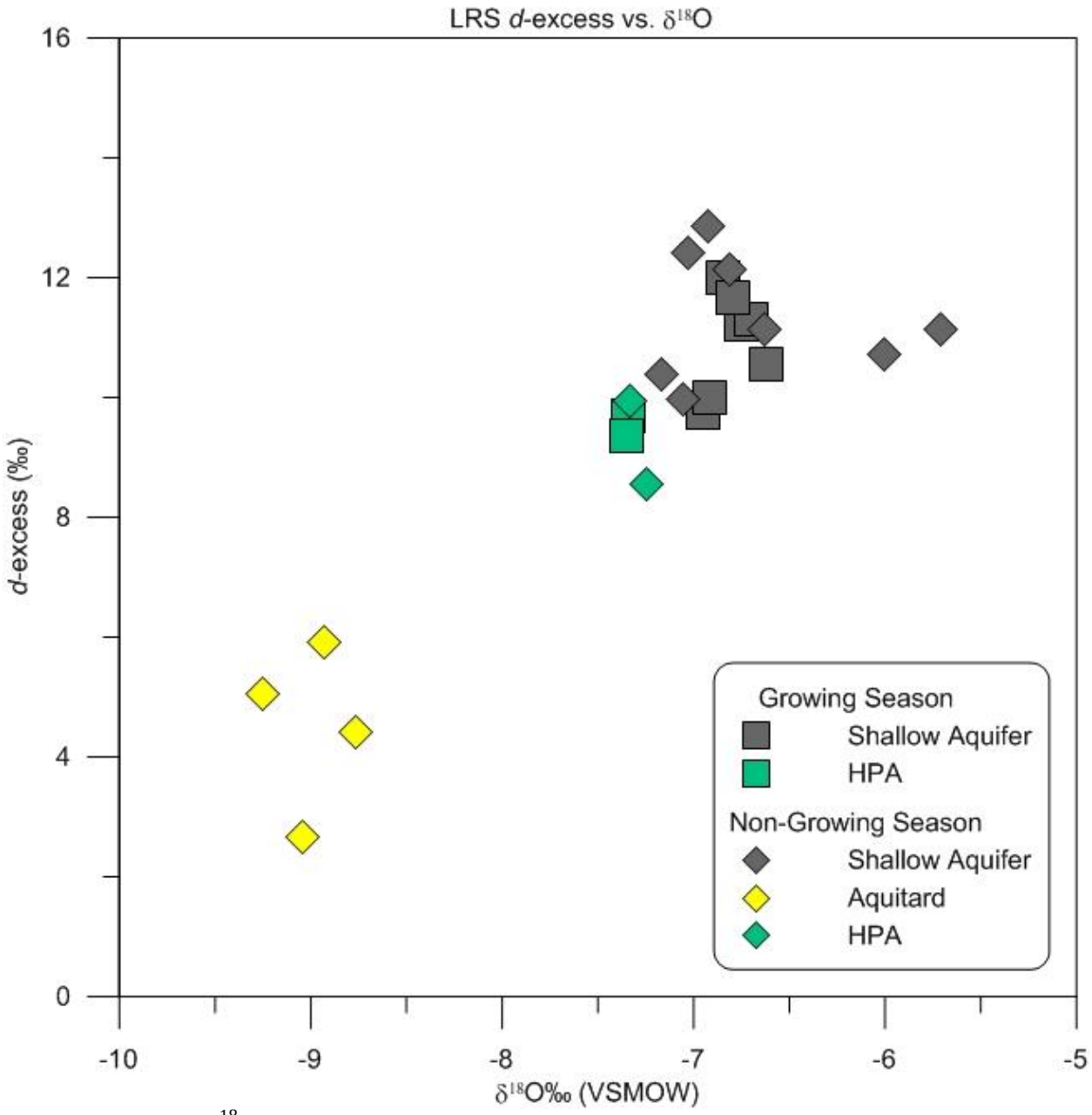


Figure 29. Plot of $\delta^{18}O$ vs. *d*-excess measurements from all sampling events at the LRS.

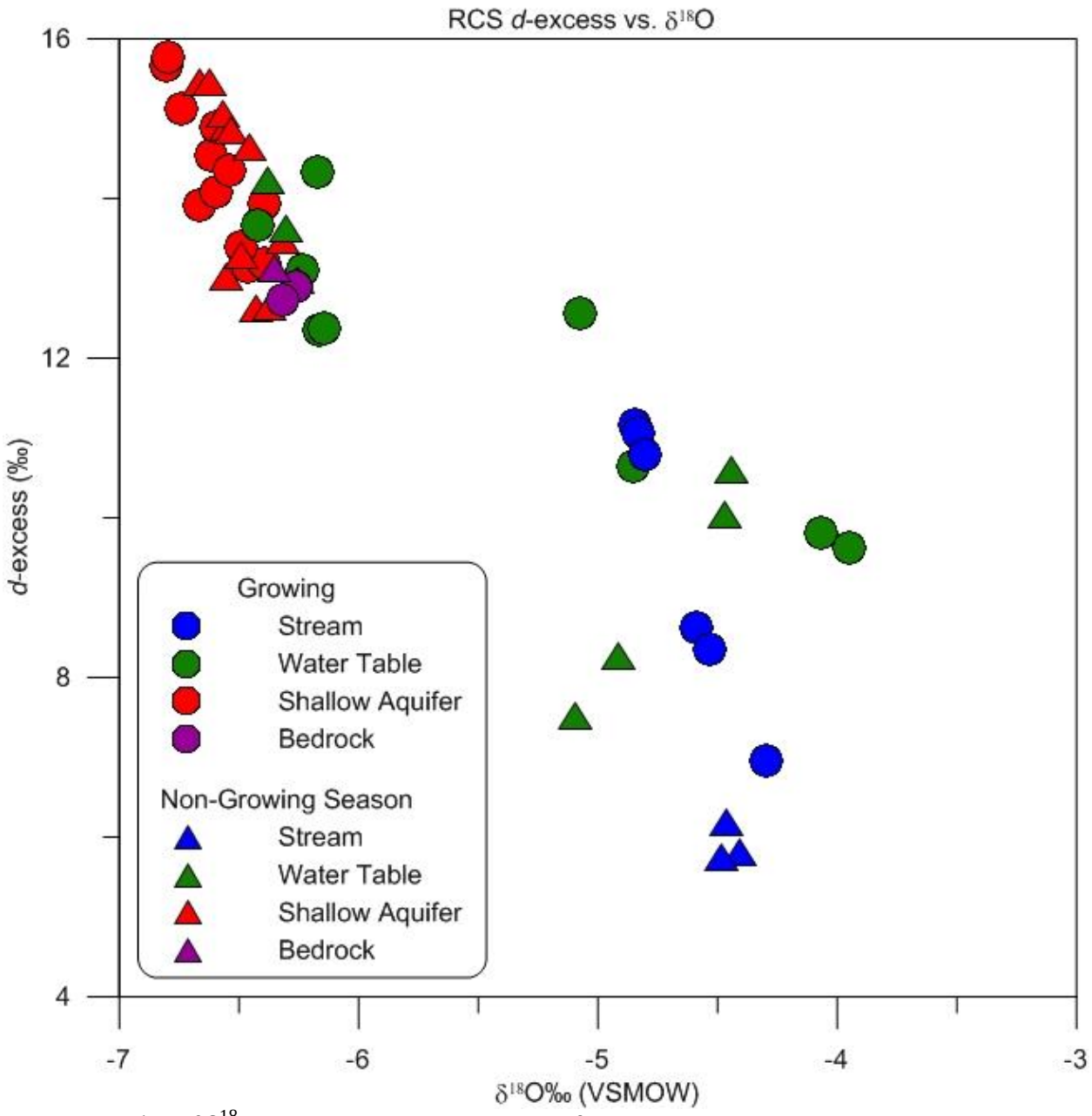

Figure 30. Plot of $\delta^{18}O$ vs. *d*-excess measurements from all sampling events at the RCS.

Table 5. Groundwater field and geochemical data for the LRS. Specific conductance is abbreviated as Sp. C. Duplicate samples at each individual well were averaged.

**LRS Growing Season**

| Sample ID | Field Sp. C. (µS/cm) | Lab Sp. C. (µS/cm) | Lab pH | $SiO_2$ (mg/L) | Ca (mg/L) | Mg (mg/L) | Na (mg/L) | K (mg/L) | Sr (mg/L) | $HCO_3$ (mg/L) | $SO_4$ (mg/L) | Cl (mg/L) | F (mg/L) | $NO_3$ (mg/L) | $NO_3$-N (mg/L) | Br (mg/L) | B (mg/L) | TDS (mg/L) |
|---|---|---|---|---|---|---|---|---|---|---|---|---|---|---|---|---|---|---|
| *Samples collected on June 7, 2013* | | | | | | | | | | | | | | | | | | |
| LWPH6 | 1839 | 1852 | 7.20 | 17.0 | 228.1 | 41.9 | 134.7 | 6.08 | 1.89 | 337 | 581.1 | 89.5 | 0.66 | 72.14 | 16.30 | 0.15 | 0.115 | 1339 |
| LWPH4A | 1734 | 1753 | 7.05 | 16.9 | 217.7 | 39.3 | 126.8 | 5.72 | 1.82 | 317 | 550.6 | 84.7 | 0.62 | 73.02 | 16.50 | 0.11 | 0.119 | 1273 |
| LWPH4B | 1707 | 1721 | 7.05 | 18.3 | 215.0 | 40.8 | 116.8 | 5.69 | 1.69 | 322 | 524.4 | 84.3 | 0.39 | 57.07 | 12.89 | 0.15 | 0.117 | 1223 |
| LWPH4C | 1295 | 1314 | 7.10 | 17.9 | 140.9 | 26.6 | 104.4 | 5.42 | 1.11 | 241 | 372.1 | 73.3 | 0.32 | 23.55 | 5.32 | 0.09 | 0.087 | 884 |
| *Samples collected on July 11, 2013* | | | | | | | | | | | | | | | | | | |
| LWPH6 | 1840 | 1894 | 7.20 | 18.6 | 242.1 | 43.9 | 141.5 | 6.67 | 1.97 | 338 | 571.7 | 89.4 | 0.56 | 71.26 | 16.10 | 0.18 | 0.113 | 1354 |
| LWPH3 | 1876 | 1918 | 7.13 | 17.8 | 244.3 | 42.2 | 151.5 | 7.71 | 2.04 | 325 | 594.8 | 100.9 | 0.66 | 70.80 | 15.99 | 0.15 | 0.103 | 1393 |
| LWPH4A | 1661 | 1760 | 7.18 | 18.1 | 221.1 | 39.6 | 128.4 | 6.41 | 1.83 | 307 | 523.3 | 81.6 | 0.61 | 69.77 | 15.76 | 0.16 | 0.108 | 1242 |
| LWPH4B | 1676 | 1737 | 7.15 | 19.2 | 223.2 | 42.1 | 120.6 | 5.85 | 1.72 | 322 | 521.0 | 81.7 | 0.36 | 56.08 | 12.67 | 0.15 | 0.098 | 1231 |
| LWPH4C | 1271 | 1318 | 7.20 | 18.7 | 148.4 | 27.4 | 105.4 | 5.71 | 1.14 | 241 | 363.5 | 70.9 | 0.30 | 21.02 | 4.75 | 0.11 | 0.082 | 881 |

**LRS Non-Growing Season**

| Sample ID | Field Sp. C. (µS/cm) | Lab Sp. C. (µS/cm) | Lab pH | $SiO_2$ (mg/L) | Ca (mg/L) | Mg (mg/L) | Na (mg/L) | K (mg/L) | Sr (mg/L) | $HCO_3$ (mg/L) | $SO_4$ (mg/L) | Cl (mg/L) | F (mg/L) | $NO_3$ (mg/L) | $NO_3$-N (mg/L) | Br (mg/L) | B (mg/L) | TDS (mg/L) |
|---|---|---|---|---|---|---|---|---|---|---|---|---|---|---|---|---|---|---|
| *Samples collected on November 19, 2012* | | | | | | | | | | | | | | | | | | |
| LWPH6 | 1733 | 1753 | 6.78 | 17.0 | 217.2 | 40.1 | 121.3 | 6.16 | 1.74 | 322 | 518.7 | 85.3 | 0.73 | 72.42 | 16.36 | 0.18 | 0.111 | 1239 |
| LWPH4A | 1707 | 1732 | 6.71 | 17.4 | 211.5 | 38.8 | 118.9 | 6.10 | 1.78 | 327 | 504.2 | 83.0 | 0.67 | 72.53 | 16.38 | 0.19 | 0.119 | 1216 |
| LWPH4B | 1665 | 1699 | 6.87 | 18.2 | 210.6 | 40.6 | 111.3 | 5.82 | 1.61 | 311 | 504.8 | 88.8 | 0.41 | 56.80 | 12.83 | 0.17 | 0.102 | 1192 |
| LWCB1 | 616 | 603 | 6.65 | 19.0 | 70.4 | 11.7 | 36.3 | 3.21 | 0.54 | 191 | 104.9 | 23.1 | 0.50 | 3.96 | 0.89 | 0.05 | 0.047 | 368 |
| LWCB2 | 602 | 620 | 6.93 | 17.7 | 70.1 | 12.1 | 39.7 | 3.92 | 0.57 | 186 | 85.3 | 38.8 | 0.49 | 8.59 | 1.94 | 0.07 | 0.046 | 369 |
| LWPH4C | 1260 | 1288 | 6.82 | 18.2 | 139.7 | 26.0 | 99.2 | 5.96 | 1.04 | 237 | 350.2 | 75.1 | 0.36 | 22.23 | 5.02 | 0.16 | 0.089 | 855 |
| *Samples collected on October 15, 2013* | | | | | | | | | | | | | | | | | | |
| LWPH6 | 1857 | 1819 | 6.87 | 17.0 | 227.6 | 40.5 | 133.7 | 6.84 | 1.88 | 325 | 535.9 | 81.0 | 0.59 | 78.68 | 17.77 | 0.17 | 0.119 | 1284 |
| LWPH3 | 1920 | 1889 | 7.08 | 20.3 | 244.2 | 42.6 | 133.2 | 7.58 | 2.13 | 376 | 558.5 | 82.7 | 0.58 | 73.70 | 16.65 | 0.14 | 0.136 | 1350 |
| LWPH4A | 1424 | 1388 | 7.23 | 17.1 | 161.7 | 28.6 | 102.1 | 5.52 | 1.36 | 267 | 386.2 | 59.3 | 0.70 | 46.60 | 10.53 | 0.09 | 0.107 | 941 |
| LWPH2 | 1436 | 1403 | 7.25 | 18.4 | 180.4 | 30.6 | 96.5 | 6.31 | 1.49 | 242 | 424.7 | 59.4 | 0.65 | 31.70 | 7.16 | 0.10 | 0.098 | 969 |
| LWPH4B | 1721 | 1678 | 7.24 | 17.9 | 206.3 | 39.0 | 113.5 | 5.74 | 1.60 | 318 | 502.8 | 76.8 | 0.42 | 52.09 | 11.77 | 0.13 | 0.098 | 1172 |
| LWCB1 | | 609 | 7.71 | 17.5 | 67.9 | 11.6 | 36.8 | 3.56 | 0.57 | 186 | 83.0 | 35.9 | 0.48 | 8.23 | 1.86 | 0.06 | 0.044 | 357 |
| LWCB2 | | 579 | 7.78 | 18.3 | 64.6 | 10.9 | 34.4 | 3.00 | 0.53 | 192 | 99.1 | 19.8 | 0.39 | 2.09 | 0.47 | 0.05 | 0.044 | 348 |
| LWPH4C | 1342 | 1302 | 6.93 | 16.9 | 138.6 | 25.9 | 101.9 | 5.09 | 1.11 | 239 | 361.6 | 69.1 | 0.30 | 24.49 | 5.53 | 0.13 | 0.088 | 862 |

Table 6. Surface and groundwater field and geochemical data for the RCS. Specific conductance is abbreviated as Sp. C. Duplicate samples at each individual well were averaged.

**RCS Growing Season**

| Sample ID | Field Sp. C. (µS/cm) | Lab pH | Si (mg/L) | $SiO_2$ (mg/L) | Ca (mg/L) | Mg (mg/L) | Na (mg/L) | K (mg/L) | Sr (mg/L) | B (mg/L) | $HCO_3$ (mg/L) | Cl (mg/L) | $SO_4$ (mg/L) | $NO_3$ (mg/L) | $NO_3$-N (mg/L) | F (mg/L) | Br (mg/L) | TDS (mg/L) |
|---|---|---|---|---|---|---|---|---|---|---|---|---|---|---|---|---|---|---|
| *Samples collected June 6, 2013* | | | | | | | | | | | | | | | | | | |
| Upstream | 1377 | 7.60 | 7.28 | 15.6 | 115.1 | 35.7 | 113.2 | 4.96 | 1.27 | 0.073 | 284 | 207.7 | 144.5 | 0.36 | 0.08 | 0.18 | 0.77 | 779 |
| Middle Stream | 1304 | 7.65 | 7.21 | 15.4 | 111.1 | 34.8 | 103.5 | 5.12 | 1.24 | 0.070 | 285 | 193.0 | 133.9 | 0.35 | 0.08 | 0.18 | 0.61 | 739 |
| Downstream | 1257 | 7.65 | 7.07 | 15.1 | 107.4 | 34.1 | 97.2 | 5.20 | 1.22 | 0.070 | 273 | 183.6 | 127.8 | 0.35 | 0.08 | 0.17 | 0.57 | 707 |
| Well B-WT | 2101 | 7.20 | 9.42 | 20.2 | 196.6 | 56.4 | 198.0 | 1.44 | 1.35 | 0.063 | 445 | 306.0 | 307.8 | 0.09 | 0.02 | 0.30 | 1.16 | 1308 |
| Well C-WT | 3309 | 7.08 | 11.53 | 24.7 | 308.7 | 80.9 | 307.4 | 0.96 | 1.81 | 0.038 | 397 | 637.4 | 504.0 | 0.09 | 0.02 | 0.27 | 2.13 | 2064 |
| Well D-WT | 2029 | | 5.36 | 11.5 | 219.6 | 45.5 | 116.1 | 1.84 | 0.95 | 0.021 | | 469.6 | 111.4 | 8.14 | 1.84 | 0.19 | 1.81 | |
| Well E-WT | 2086 | 7.00 | 9.92 | 21.2 | 209.9 | 48.0 | 166.9 | 1.25 | 0.98 | 0.010 | 458 | 364.4 | 171.3 | 0.36 | 0.08 | 0.25 | 1.29 | 1211 |
| Well A | 1310 | 7.08 | 9.96 | 21.3 | 132.0 | 42.9 | 77.8 | 1.33 | 1.69 | 0.033 | 383 | 164.8 | 120.1 | 0.51 | 0.11 | 0.26 | 0.55 | 752 |
| Well B | 1354 | 7.08 | 10.06 | 21.5 | 134.6 | 43.6 | 81.9 | 1.40 | 1.78 | 0.035 | 384 | 172.3 | 123.1 | 0.72 | 0.16 | 0.26 | 0.63 | 770 |
| Well C | 1167 | 7.45 | 8.62 | 18.4 | 133.3 | 37.1 | 51.1 | 1.39 | 0.61 | 0.062 | 344 | 155.9 | 79.3 | 0.20 | 0.05 | 0.19 | 0.59 | 647 |
| Well D | 1487 | 7.20 | 9.96 | 21.3 | 143.2 | 49.1 | 93.6 | 1.50 | 2.21 | 0.043 | 378 | 209.9 | 141.3 | 0.67 | 0.15 | 0.27 | 0.83 | 850 |
| Well E | 1032 | 7.33 | 9.71 | 20.8 | 118.3 | 31.9 | 50.2 | 1.22 | 0.58 | 0.026 | 380 | 101.6 | 70.6 | 0.09 | 0.02 | 0.20 | 0.40 | 583 |
| Well F | 1052 | 7.15 | 9.96 | 21.3 | 113.0 | 34.2 | 58.8 | 1.22 | 1.20 | 0.027 | 392 | 97.4 | 77.5 | 1.29 | 0.29 | 0.28 | 0.38 | 599 |
| Well H | 1730 | 7.30 | 8.59 | 18.4 | 121.7 | 60.7 | 148.0 | 1.72 | 5.46 | 0.081 | 354 | 265.1 | 200.9 | 0.18 | 0.04 | 0.83 | 1.16 | 998 |
| *Samples collected September 2, 2013* | | | | | | | | | | | | | | | | | | |
| Upstream | 953 | 7.93 | 7.43 | 15.9 | 91.9 | 28.7 | 62.3 | 4.88 | 0.90 | 0.063 | 268 | 115.5 | 96.9 | 0.79 | 0.18 | 0.15 | 0.38 | 550 |
| Middle Stream | 961 | 7.92 | 7.59 | 16.3 | 88.1 | 27.5 | 60.8 | 4.44 | 0.96 | 0.059 | 261 | 118.0 | 98.0 | 0.75 | 0.17 | 0.15 | 0.40 | 544 |
| Downstream | 972 | 7.98 | 7.43 | 15.9 | 90.0 | 28.8 | 63.3 | 4.43 | 0.95 | 0.062 | 258 | 120.6 | 97.8 | 0.69 | 0.16 | 0.15 | 0.41 | 550 |
| B-WT | 3461 | 6.93 | 12.15 | 26.0 | 348.5 | 92.3 | 277.3 | 1.82 | 2.35 | 0.089 | 435 | 698.7 | 467.2 | 0.06 | 0.01 | 0.27 | 2.12 | 2131 |
| C-WT | 3047 | 7.02 | 12.16 | 26.1 | 282.6 | 72.8 | 272.8 | 0.87 | 1.69 | 0.079 | 407 | 609.8 | 355.3 | 0.00 | 0.00 | 0.28 | 1.85 | 1824 |
| D-WT | 2142 | 7.23 | 9.72 | 20.8 | 212.3 | 44.3 | 151.4 | 1.97 | 0.94 | 0.050 | 256 | 487.4 | 131.1 | 6.09 | 1.38 | 0.19 | 1.60 | 1184 |
| E-WT | 2716 | 6.84 | 11.05 | 23.7 | 280.0 | 65.1 | 213.2 | 1.14 | 1.29 | 0.065 | 457 | 531.1 | 244.3 | 0.08 | 0.02 | 0.22 | 1.60 | 1587 |
| F-WT | 3688 | 6.86 | 8.79 | 18.8 | 359.4 | 102.7 | 286.7 | 1.28 | 1.51 | 0.027 | 395 | 825.5 | 406.3 | 0.11 | 0.03 | 0.15 | 2.42 | 2199 |
| Well A | 1273 | 7.17 | 10.32 | 22.1 | 131.3 | 41.6 | 74.5 | 1.26 | 1.73 | 0.044 | 378 | 156.4 | 118.3 | 0.49 | 0.11 | 0.28 | 0.57 | 734 |
| Well B | 1351 | 7.14 | 9.86 | 21.1 | 132.4 | 42.2 | 78.3 | 1.37 | 1.74 | 0.048 | 376 | 175.9 | 125.6 | 0.59 | 0.13 | 0.27 | 0.62 | 765 |
| Well C | 1160 | 7.18 | 8.82 | 18.9 | 129.7 | 35.9 | 48.2 | 1.35 | 0.63 | 0.148 | 353 | 151.4 | 73.6 | 0.29 | 0.07 | 0.19 | 0.51 | 634 |
| Well D | 1457 | 7.10 | 9.96 | 21.4 | 141.4 | 47.3 | 88.6 | 1.39 | 2.19 | 0.048 | 379 | 204.1 | 139.1 | 0.54 | 0.12 | 0.27 | 0.71 | 833 |
| Well E | 1016 | 7.16 | 9.77 | 20.9 | 109.7 | 32.3 | 55.3 | 1.19 | 1.13 | 0.035 | 386 | 92.1 | 72.5 | 1.27 | 0.29 | 0.27 | 0.31 | 577 |
| Well F | 1016 | 7.18 | 10.06 | 21.6 | 118.9 | 31.1 | 50.4 | 1.17 | 0.61 | 0.030 | 383 | 97.6 | 70.4 | 0.23 | 0.05 | 0.19 | 0.33 | 581 |
| Well H | 1714 | 7.16 | 8.56 | 18.3 | 122.4 | 60.6 | 146.7 | 1.65 | 5.58 | 0.093 | 349 | 265.0 | 200.6 | 0.05 | 0.01 | 0.85 | 1.01 | 994 |

Table 6. Continued.

**RCS Non-Growing Season**

| Sample ID | Field Sp. C. (µS/cm) | Lab pH | Si (mg/L) | $SiO_2$ (mg/L) | Ca (mg/L) | Mg (mg/L) | Na (mg/L) | K (mg/L) | Sr (mg/L) | B (mg/L) | $HCO_3$ (mg/L) | Cl (mg/L) | $SO_4$ (mg/L) | $NO_3$ (mg/L) | $NO_3$-N (mg/L) | F (mg/L) | Br (mg/L) | TDS (mg/L) |
|---|---|---|---|---|---|---|---|---|---|---|---|---|---|---|---|---|---|---|
| *Samples collected April 16, 2013* | | | | | | | | | | | | | | | | | | |
| Upstream | 1820 | 8.04 | 4.40 | 9.4 | 162.2 | 60.2 | 146.1 | 3.03 | 1.89 | 0.078 | 361 | 265.4 | 271.9 | 0.00 | 0.00 | 0.22 | 0.93 | 1099 |
| Middle Stream | 1800 | 8.00 | 4.45 | 9.5 | 162.3 | 60.2 | 147.2 | 3.03 | 1.90 | 0.079 | 353 | 270.2 | 300.7 | 0.00 | 0.00 | 0.22 | 0.89 | 1130 |
| Downstream | 1822 | 7.97 | 4.44 | 9.5 | 163.0 | 60.2 | 147.4 | 3.01 | 1.87 | 0.080 | 371 | 270.9 | 296.0 | 0.00 | 0.00 | 0.22 | 0.88 | 1136 |
| B-WT | 2577 | 7.10 | 9.18 | 19.7 | 244.4 | 66.2 | 240.5 | 1.13 | 1.54 | 0.030 | 361 | 388.8 | 512.6 | 0.19 | 0.03 | 0.31 | 1.29 | 1654 |
| C-WT | 2676 | 7.09 | 11.09 | 23.8 | 246.5 | 61.1 | 277.2 | 0.59 | 1.35 | 0.026 | 394 | 392.1 | 538.3 | 0.00 | 0.00 | 0.30 | 1.29 | 1736 |
| D-WT | 2021 | 7.42 | 8.29 | 17.8 | 221.0 | 45.1 | 116.9 | 1.87 | 0.94 | 0.026 | 228 | 437.5 | 111.3 | 12.82 | 2.24 | 0.16 | 1.61 | 1079 |
| E-WT | 1874 | 7.07 | 9.94 | 21.3 | 194.4 | 47.0 | 141.3 | 0.93 | 0.93 | 0.011 | 510 | 301.5 | 91.8 | 0.03 | 0.00 | 0.23 | 1.13 | 1051 |
| Well A | 1347 | 7.07 | 10.23 | 21.9 | 138.0 | 43.7 | 78.9 | 1.53 | 1.75 | 0.041 | 379 | 176.3 | 118.9 | 0.49 | 0.10 | 0.26 | 0.60 | 769 |
| Well B | 1358 | 7.11 | 10.32 | 22.1 | 140.4 | 44.0 | 82.7 | 1.38 | 1.77 | 0.037 | 377 | 177.4 | 119.9 | 0.64 | 0.11 | 0.25 | 0.60 | 777 |
| Well C | 1146 | 7.46 | 8.61 | 18.4 | 128.7 | 36.5 | 50.7 | 1.39 | 0.58 | 0.091 | 321 | 158.5 | 77.8 | 0.32 | 0.06 | 0.15 | 0.58 | 631 |
| Well D | 1499 | 7.09 | 10.41 | 22.3 | 151.8 | 50.6 | 96.5 | 1.53 | 2.30 | 0.038 | 376 | 216.2 | 138.8 | 0.59 | 0.10 | 0.30 | 0.75 | 866 |
| Well E | 1069 | 7.09 | 10.58 | 22.7 | 119.6 | 35.2 | 60.7 | 1.18 | 1.24 | 0.023 | 392 | 102.7 | 78.2 | 1.26 | 0.22 | 0.25 | 0.36 | 616 |
| Well F | 982 | 7.28 | 10.02 | 21.5 | 119.3 | 31.6 | 47.6 | 1.09 | 0.54 | 0.021 | 371 | 101.1 | 60.2 | 0.12 | 0.02 | 0.18 | 0.37 | 566 |
| Well H | 1677 | 7.20 | 8.94 | 19.2 | 126.7 | 61.3 | 151.2 | 1.72 | 5.51 | 0.083 | 353 | 252.2 | 208.4 | 0.29 | 0.05 | 0.85 | 1.11 | 1002 |
| *Samples collected November 7, 2013* | | | | | | | | | | | | | | | | | | |
| Upstream | 626 | 7.46 | 5.81 | 12.5 | 62.3 | 19.0 | 37.5 | 6.72 | 0.27 | 0.047 | 178 | 73.5 | 53.5 | 0.98 | 0.22 | 0.16 | 0.20 | 354 |
| Middle Stream | 620 | 7.48 | 5.75 | 12.3 | 61.3 | 18.7 | 36.5 | 6.74 | 0.27 | 0.046 | 179 | 72.4 | 52.7 | 1.04 | 0.24 | 0.15 | 0.21 | 350 |
| Downstream | 618 | 7.51 | 5.70 | 12.2 | 61.0 | 18.5 | 36.0 | 6.65 | 0.26 | 0.046 | 178 | 72.1 | 52.3 | 1.01 | 0.23 | 0.16 | 0.20 | 348 |
| B-WT | 2768 | 6.97 | 12.46 | 26.7 | 277.2 | 75.5 | 237.7 | 1.89 | 0.84 | 0.100 | 452 | 541.9 | 321.7 | 0.11 | 0.02 | 0.29 | 1.64 | 1707 |
| C-WT | 2494 | 7.04 | 13.48 | 28.9 | 242.2 | 64.6 | 224.8 | 1.10 | 0.67 | 0.090 | 457 | 469.8 | 260.7 | 0.03 | 0.01 | 0.28 | 1.45 | 1519 |
| D-WT | 2109 | 7.19 | 9.04 | 19.4 | 234.4 | 47.4 | 135.4 | 2.02 | 0.45 | 0.031 | 264 | 492.5 | 114.0 | 4.82 | 1.09 | 0.16 | 1.54 | 1182 |
| E-WT | 2598 | 6.86 | 11.59 | 24.8 | 279.5 | 62.2 | 213.5 | 1.19 | 0.57 | 0.019 | 497 | 519.0 | 215.3 | 0.04 | 0.01 | 0.22 | 1.49 | 1562 |
| Well A | 1270 | 7.16 | 10.77 | 23.1 | 131.3 | 42.9 | 77.7 | 1.36 | 0.78 | 0.036 | 379 | 165.3 | 116.5 | 0.47 | 0.11 | 0.33 | 0.52 | 747 |
| Well B | 1395 | 7.04 | 10.46 | 22.4 | 142.2 | 46.6 | 88.9 | 1.41 | 0.86 | 0.039 | 375 | 199.9 | 131.2 | 0.53 | 0.12 | 0.33 | 0.63 | 819 |
| Well C | 1139 | 7.22 | 9.24 | 19.8 | 132.7 | 37.6 | 51.3 | 1.39 | 0.28 | 0.154 | 357 | 157.6 | 69.7 | 0.29 | 0.06 | 0.18 | 0.49 | 647 |
| Well D | 1495 | 7.16 | 10.31 | 22.1 | 148.5 | 51.0 | 97.2 | 1.51 | 1.05 | 0.042 | 375 | 229.1 | 143.3 | 0.55 | 0.12 | 0.30 | 0.71 | 879 |
| Well E | 1018 | 7.21 | 10.47 | 22.4 | 113.3 | 34.2 | 59.5 | 1.24 | 0.53 | 0.027 | 389 | 101.0 | 72.8 | 1.33 | 0.30 | 0.32 | 0.30 | 598 |
| Well F | 1010 | 7.28 | 10.25 | 22.0 | 118.9 | 32.4 | 52.7 | 1.21 | 0.27 | 0.030 | 377 | 105.7 | 70.6 | 0.21 | 0.05 | 0.23 | 0.33 | 590 |
| Well H | 1722 | 7.23 | 8.89 | 19.0 | 124.8 | 62.8 | 152.8 | 1.75 | 2.57 | 0.088 | 350 | 277.0 | 192.7 | 0.12 | 0.03 | 0.78 | 0.95 | 1007 |

Table 7. Groundwater isotopic data for the LRS. Duplicate samples at each individual well were averaged. Deuterium excess, *d*-excess, was calculated by the following equation: *d*-excess = 8* $\delta^{18}O + 10$.

**LRS Growing Season**

| Sample ID | $\delta^{18}O$‰ (VSMOW) | $\delta^{2}H$‰ (VSMOW) | *d*-excess (‰) |
|---|---|---|---|
| *Samples Collected on June 7, 2013* | | | |
| LWPH6 | -6.8 | -43 | 12.0 |
| LWPH4A | -6.6 | -42 | 10.5 |
| LWPH4B | -6.9 | -46 | 9.7 |
| LWPH4C | -7.3 | -49 | 9.7 |
| *Samples Collected on July 11, 2013* | | | |
| LWPH6 | -6.8 | -43 | 11.7 |
| LWPH3 | -6.7 | -42 | 11.3 |
| LWPH4A | -6.7 | -43 | 11.2 |
| LWPH4B | -6.9 | -45 | 10.0 |
| LWPH4C | -7.3 | -49 | 9.3 |

**LRS Non-Growing Season**

| Sample ID | $\delta^{18}O$‰ (VSMOW) | $\delta^{2}H$‰ (VSMOW) | *d*-excess (‰) |
|---|---|---|---|
| *Samples Collected on November 19, 2012* | | | |
| LWPH6 | -7.0 | -44 | 12.4 |
| LWPH4A | -6.8 | -42 | 12.1 |
| LWPH4B | -7.2 | -47 | 10.4 |
| LWCB1 | -9.3 | -69 | 5.1 |
| LWCB2 | -8.9 | -65 | 5.9 |
| LWPH4C | -7.3 | -49 | 9.9 |
| *Samples Collected on October 15, 2013* | | | |
| LWPH6 | -6.9 | -43 | 12.8 |
| LWPH3 | -6.6 | -42 | 11.1 |
| LWPH4A | -6.0 | -37 | 10.7 |
| LWPH2 | -5.7 | -35 | 11.1 |
| LWPH4B | -7.1 | -46 | 10.0 |
| LWCB1 | -8.8 | -66 | 4.4 |
| LWCB2 | -9.0 | -70 | 2.7 |
| LWPH4C | -7.2 | -49 | 8.5 |

Table 8. Surface and groundwater isotopic data for the RCS. Duplicate samples at each individual well were averaged. Deuterium excess, *d*-excess, was calculated by the following equation: *d*-excess = 8* $\delta^{18}O$ + 10.

**RCS Growing Season**

| Sample ID | $\delta^{18}O$‰ (VSMOW) | $\delta^{2}H$‰ (VSMOW) | *d*-excess (‰) |
|---|---|---|---|
| *Samples collected on June 13, 2013* | | | |
| Upstream | -4.6 | -28 | 8.6 |
| Mid-Stream | -4.5 | -28 | 8.3 |
| Downstream | -4.3 | -27 | 7.0 |
| B-WT | -5.1 | -28 | 12.6 |
| C-WT | -4.9 | -28 | 10.6 |
| D-WT | -6.2 | -37 | 12.4 |
| E-WT | -6.1 | -37 | 12.4 |
| Well A | -6.6 | -38 | 14.5 |
| Well B | -6.7 | -39 | 15.1 |
| Well C | -6.8 | -39 | 15.7 |
| Well D | -6.5 | -39 | 13.1 |
| Well E | -6.4 | -38 | 13.2 |
| Well F | -6.4 | -37 | 13.9 |
| Well H | -6.3 | -37 | 12.9 |
| *Samples collected on September 2, 2013* | | | |
| Upstream | -4.8 | -28 | 11.2 |
| Mid-Stream | -4.8 | -28 | 11.1 |
| Downstream | -4.8 | -28 | 10.8 |
| B-WT | -4.1 | -23 | 9.8 |
| C-WT | -4.0 | -22 | 9.6 |
| D-WT | -6.4 | -38 | 13.7 |
| E-WT | -6.2 | -35 | 14.3 |
| F-WT | -6.2 | -37 | 13.1 |
| Well A | -6.7 | -39 | 13.9 |
| Well B | -6.6 | -39 | 14.1 |
| Well C | -6.5 | -39 | 13.4 |
| Well D | -6.5 | -38 | 14.4 |
| Well E | -6.6 | -38 | 14.9 |
| Well F | -6.8 | -39 | 15.8 |
| Well H | -6.3 | -38 | 12.7 |

**RCS Non-Growing Season**

| Sample ID | $\delta^{18}O$‰ (VSMOW) | $\delta^{2}H$‰ (VSMOW) | *d*-excess (‰) |
|---|---|---|---|
| *Samples collected on April 16, 2013* | | | |
| Upstream | -4.5 | -30 | 6.2 |
| Mid-Stream | -4.4 | -29 | 5.8 |
| Downstream | -4.5 | -30 | 5.8 |
| B-WT | -5.1 | -33 | 7.5 |
| C-WT | -4.9 | -31 | 8.3 |
| D-WT | -6.3 | -37 | 13.6 |
| E-WT | -6.3 | -37 | 13.0 |
| Well A | -6.7 | -38 | 15.5 |
| Well B | -6.6 | -39 | 13.0 |
| Well C | -6.4 | -39 | 12.6 |
| Well D | -6.5 | -39 | 13.3 |
| Well E | -6.3 | -37 | 13.5 |
| Well F | -6.4 | -38 | 12.7 |
| Well H | -6.4 | -38 | 13.1 |
| *Samples collected on November 7, 2013* | | | |
| B-WT | -4.5 | -26 | 10.0 |
| C-WT | -4.4 | -25 | 10.6 |
| D-WT | -6.4 | -37 | 14.2 |
| Well A | -6.6 | -38 | 15.5 |
| Well B | -6.6 | -38 | 14.9 |
| Well C | -6.6 | -37 | 15.1 |
| Well D | -6.5 | -37 | 14.9 |
| Well E | -6.5 | -37 | 14.7 |

Table 9. Relative annual and seasonal average precipitation isotope compositions were determined by the Online Isotopes Precipitation Calculator (Bowen and Revenaugh, 2003; Bowen et al., 2005; OIPC, 2014). The summer months included June, July, and August; the spring months included March, April, and May; the fall months included September, October, and November; and the winter months included December, January, and February.

**LRS Precipitation**

| | $\delta^{18}O‰$ (VSMOW) | $\delta^{2}H‰$ (VSMOW) |
|---|---|---|
| *Monthly Average* | | |
| January | -110 | -15 |
| February | -94 | -13.1 |
| March | -71 | -9.9 |
| April | -58 | -8.6 |
| May | -55 | -7.6 |
| June | -55 | -7.5 |
| July | -45 | -6.1 |
| August | -46 | -6.2 |
| September | -62 | -9 |
| October | -65 | -9.6 |
| November | -81 | -11.5 |
| December | -97 | -13.8 |
| *Seasonal Average* | | |
| Fall | -69 | -10.0 |
| Winter | -100 | -14.0 |
| Spring | -61 | -8.7 |
| Summer | -49 | -6.6 |
| *Annual Average* | | |
| | -61 | -8.5 |

**RCS Precipitation**

| | $\delta^{18}O‰$ (VSMOW) | $\delta^{2}H‰$ (VSMOW) |
|---|---|---|
| *Monthly Average* | | |
| January | -88 | -12.2 |
| February | -76 | -10.8 |
| March | -53 | -7.6 |
| April | -43 | -6.6 |
| May | -42 | -5.7 |
| June | -43 | -5.9 |
| July | -32 | -4.4 |
| August | -34 | -4.5 |
| September | -50 | -7.4 |
| October | -51 | -7.9 |
| November | -65 | -9.3 |
| December | -80 | -11.5 |
| *Seasonal Average* | | |
| Fall | -55 | -8.2 |
| Winter | -81 | -11.5 |
| Spring | -46 | -6.6 |
| Summer | -36 | -4.9 |
| *Annual Average* | | |
| | -50 | -7.1 |